LUND UNIVERSITY

Comparison of chemical properties of iron, cobalt, and nickel porphyrins, corrins, and hydrocorphins

Jensen, Kasper; Ryde, Ulf

Comparison of chemical properties of iron, cobalt, and nickel porphyrins, corrins, and hydrocorphins

Kasper P. Jensen and Ulf Ryde*

Department of Theoretical Chemistry

Lund University

Chemical Centre

P. O. Box 124

S-221 00 Lund

Sweden

Correspondence to Ulf Ryde

E-mail: Ulf.Ryde@teokem.lu.se

Tel: +46 – 46 2224502

Fax: +46 – 46 2224543

2017-04-09

Density functional calculations have been used to compare the geometric, electronic, and functional properties of the three important tetrapyrrole systems in biology, haem, coenzyme B_{12}, and coenzyme F430, which are formed by iron porphyrin (Por), cobalt corrin (Cor), and nickel hydrocorphin (Hcor). The results show that the flexibility of the ring systems follows the trend Hcor > Cor > Por and that the size of the central cavity follows the trend Cor < Por < Hcor. Therefore, low-spin Co^{I}, Co^{II}, and Co^{III} fit well into the Cor ring, whereas Por seems to be more ideal for the higher spin states of iron, and the cavity in Hcor is tailored for the larger Ni ion, especially in the high-spin Ni^{II} state. This is confirmed by the thermodynamic stabilities of the various combinations of metals and ring systems,. Reduction potentials indicate that the +I and +III states are less stable for Ni than for the other metal ions. Moreover, Ni–C bonds are appreciably less stable than for Co. However, it is still possible that a $Ni–CH_3$ bond is formed in F430 by a heterolytic methyl transfer reaction, provided that the donor is appropriate, e.g. if coenzyme M is protonated. This can be facilitated by the adjacent SO_3^- group in this coenzyme and by the axial glutamine ligand, which stabilises the Ni^{III} state. Our results also show that a $Ni^{III}–CH_3$ complex is readily hydrolysed to form a methane molecule and that the Ni^{III} hydrolysis product can oxidise coenzyme B and M to a heterodisulphide in the reaction mechanism of methyl coenzyme M reductase.

Introduction

The porphyrinoids or tetrapyrrole-derived macrocycles constitute a group of important tetradentate ligands used by nature to encapsulate and utilise metals for biological function. The largest group is the haems, which consist of a protoporphyrin IX ring, binding an iron ion (cf. Figure 1). This system is central to the mixed-spin chemistry of oxygen transport (in globins) and metabolism (in haem peroxidases, catalases, P450, and many other enzymes), and also to the low-spin (LS) electron transfer during respiration.[1] The basic unit of haem is the porphine ring (Por).

Another well-known tetrapyrrole ring of a similar design is the corrin ring (Cor), which is the basic building block of cobalamins such as vitamin B_{12}. Two human enzymes, methionine synthase and methylmalonyl coenzyme A mutase use this corrin unit as a cofactor in catalysis. Corrin is responsible for the cobalt chemistry of life, in particular alkyl migration and methylation reactions.[2,3] Although the structures of Cor and Por are rather similar, they have quite differing regimes, namely mixed-spin chemistry for Por (all possible spin states) but LS chemistry for Cor.

A third tetrapyrrole of interest is the hydrocorphin ring (Hcor) found in the F430 cofactor of methyl-coenzyme M reductase (MCR). This enzyme is responsible for the terminal step in methanogenesis by anaerobic archaebacteria. The way in which the methyl group on methyl-coenzyme M is converted into methane is not yet fully understood and the spin chemistry of F430 has not been thoroughly addressed. If methyl turns out to bind directly to Ni, as is often suggested,[4,5] it would be interesting to compare the $Ni–CH_3$ bond strength with the analogous case of $Co–CH_3$ in B_{12} enzymes.

The basic ring system of the three tetrapyrroles with their native metal ions are shown in Figure 2. The porphine ring is highly symmetric, displaying D_{4h} symmetry, and contains four pyrrole rings connected by methine bridges. Corrin is similar, but it lacks one of the four methine bridges and ten carbon atoms at the periphery of the corrin ring are saturated, a feature that destroys the conjugation of the outer part of the ring. However, the metal-bound corrin ring retains C_2 symmetry. The hydrocorphin ring is asymmetric, with a large distortion of the central cavity and non-equivalent metal–N_{eq} bond distances (N_{eq} denotes the pyrrole nitrogen atoms). Two external rings connected to the tetrapyrrole skeleton, a six-membered lactone ring and a five-membered lactam ring, are responsible for this distortion. The Hcor ring is even more saturated than Cor, with only five double bonds, of which two pairs are conjugated. The porphine ring is dianionic when bound to a metal, whereas Cor and Hcor are monoanions.

1   Messerschmidt, A.; Hube, R.; Poulos, T.; Wieghart, K. (eds.), *Handbook of Metalloproteins,* John Wiley & Sons, Ltd., Chichester **2001**.
2   Glusker, J. P. *Vitamins and Hormons* **1995**, *50*, 1-76.
3   Ludwig, M. L.; Matthews, R. G. *Annu. Rev. Biochem.* **1997**, *66*, 269-313.
4   Grabarse, W.; Mahlert, F.; Duin, E. C.; Goubeaud, M.; Shima, S.; Thauer, R. K.; Lamzin, V.; Ermler, U. *J. Mol. Biol.* **2001**, *309*, 315-330.
5   Ermler, U.; Grabarse, W.; Shima, S.; Goubeaud, M.; Thauer, R. K. *Science* **1997**, *278*, 1457-1462.

Cobalt may exist in three oxidation states in vivo, Co^I, Co^{II}, and Co^{III}. The corrins usually have a d^6 LS Co^{III} ion in their octahedral resting states. Co^ICor is a very strong nucleophile, which reacts readily with most electron-deficient systems. Ni can occur in the same three oxidation states, with Ni^I being the resting state in MCR.[6] On the other hand, Fe^I is not accessible in biological chemistry (except perhaps in iron-only hydrogenases)[7], owing to the highly unfavourable reduction potential of Fe^{II}. Iron is normally encountered in the Fe^{II} or Fe^{III} states, although iron porphyrins are well-known for their accessible high-valent states (formally Fe^{IV} and Fe^V), which play important roles in the function of iron oxidases and cytochrome P450.[8,9,10]

The tetra-pyrrole ring system provides four ligands to the metal. However, in most enzymes, the metal ion also binds one or two axial ligands in an octahedral fashion. These axial ligands are believed to tune the function of the coenzyme. In most cobalamin-dependent enzymes, the imidazole side chain of a histidine (His) residue coordinates to the cobalt ion. Alternatively, cobalt may bind to the pendant dimethylbenzimidazole group of coenzyme B_{12}.[11] The second axial site is occupied by a methyl or 5'-deoxyadenosyl group, forming an organometallic Co–C bond. This bond is broken during the catalytic cycle, forming either a five-coordinate Co^{II} intermediate and an adenosyl radical, or a four-coordinate Co^I ion, where the imidazole ligand has dissociated and the methyl group has been transferred to a nucleophilic substrate.[3,12]

Haem enzymes show a larger variation in the axial ligands (His, cysteine, methionine, tyrosine, glutamate, aspartate, amino terminal, or exogenous ligands), depending on the function. The haem group can be either five-coordinate with an open coordination site, where a substrate binds, or six-coordinate with one or two ligands from the protein. However, the most common ligand is undoubtedly His, present for example in myoglobin, haemoglobin, peroxidases, haem oxygenase, and most cytochromes.

In MCR, the side chain of a glutamine (Gln) residue forms a weak bond to Ni via its oxygen atom, both in the oxidised Ni^{II} form (2.08–2.37 Å)[5] and in the active Ni^I form (2.02–2.12 Å).[13] In the crystal structures, a thiolate (2.40–2.54 Å) or the sulphonate (2.27–2.29 Å) group from coenzyme M coordinates to the Ni^{II} ion as the sixth ligand.[14] However, this does not seem to be the case in the active Ni^I form.[15]

6   Halcrow, M. A.; Christou, G. *Chem. Rev.* **1994**, *94*, 2421-2481.
7   Cao, Z.; Hall, M. B. *J. Am. Chem. Soc*. **2001**, *123*, 3734-3742.
8   Harris, D. L. *Curr. Opin. Chem. Biol.* **2001**, *5*, 724-735.
9   Fujii, H. *Coord, Chem. Rev.* **2002**, *226*, 51-60.
10 Nakamoto, K. *Coord. Chem. Rev.* **2002**, *226*, 153-165.
11 Suko, R. K.; Poppe, L.; Rétey, J.; Finke, R. G. *Bioorganic Chemistry* **1999**, *27*, 451-462.
12 Wirt, M. D.; Sagi, I.; Chance, M. R. *Biophys. J.* **1992**, *63*, 412-417.
13 Duin, E. C.; Cosper, N. J.; Mahlert, F.; Thauer, R. K.; Scott, R. A. *J. Biol. Inorg. Chem*. **2003**, *8*, 141-148.
14 Grabarse, W. G.; Mahlert, F.; Shima, S.; Thauer, R. K.; Ermler, U. *J. Mol. Biol.* **2000**, *303*, 329-344.
15 Duin, E. C.; Cosper, N. J.; Mahlert, F.; Thauer, R. K.; Scott, R. A. *J. Biol. Inorg. Chem*. **2003**, *8*, 141-148.

The three tetrapyrroles have evolved to fulfil specific functions in living organisms. Their apparent similarity and probable common ancestor, as witnessed in the biosynthesis of these compounds, raises important questions regarding how the properties of the coenzymes differ and why a certain combination of a tetrapyrrole ring and metal ion are selected in nature for a certain function. We recently started to investigate this problem from a theoretical perspective, by analysing similarities and differences in structure and function of corrin and porphine systems with iron and cobalt atoms.[16] We showed that nature has good reasons for choosing iron in porphine and cobalt in corrins. The design indicates a compromise between several functions all pointing towards the same need, namely accessible high-spin (HS) and intermediate-spin (IS) states in porphine chemistry and their absence in corrin chemistry.

The Hcor ring of cofactor F430 may differ substantially in this sense. Therefore, we here extend our study of these problems to the Ni and Hcor: Why is Ni chosen as metal in MCR? Could another metal have been chosen? Could another ring than Hcor have been used? Is the Ni–CH_3 intermediate a viable state? What significance does the axial ligand Gln have, and how strongly is it actually bound? As in our previous study,[16] we have concentrated on a typical reaction for each of the coenzymes, viz. the homo- and heterolytic breakage of the M–C bond (M denotes the metal, Ni, Co or Fe), as a typical example of coenzyme B_{12} and maybe F430 catalysis, and electron transfer, as a typical example of the haem-containing cytochromes. Our investigation is based on density functional calculations. During recent years, such methods has successfully been applied on the study of porphyrins [17,18,19,20,21,22,23,24,25,26], coenzyme B_{12} models [27,28,29,30,31,32,33,34], as well as F430 models.[35,36,37,38,39] The field of theoretical modelling of

16 Jensen, K. P.; Ryde, U. *ChemBioChem* **2003**, *4*, 413-424.
17 Spiro, T. G.; Kozlowski, P. M.; Zgierski, M. Z. *J. Raman Spectr.* **1998**, *29*, 869-879.
18 Kozlowski, P. M.; Spiro, T. G.; Bérces, A.; Zgierski, M. Z. *J. Phys. Chem. B* **1998**, *102*, 2603-2608.
19 Rovira, C.; Kunc, K.; Hutter, J.; Ballone, P.; Parinello, M. *J. Phys. Chem. A* **1997**, *101*, 8914-8925.
20 Sigfridsson, E.; Ryde, U. *J. Biol. Inorg. Chem.* **1999**, *4*, 99-110.
21 Sigfridsson, E.; Olsson, M. H. M.; Ryde, U. *J. Phys. Chem. B* **2001**, *105*, 5546-5552.
22 Green, M. T. *J. Am. Chem. Soc.* **2000**, *122*, 9495-9499.
23 Green, M. T. *J. Am. Chem. Soc.* **2001**, *123*, 9218-9219.
24 Liao, M.-S.; Scheiner, S. *J. Chem. Phys.* **2002**, *117*, 205-219.
25 Jensen, K. P.; Ryde, U. *Mol. Phys.* **2003**, *13*, 2003-2018.
26 Jensen, K. P.; Ryde, U. *J. Biol. Chem.* **2004**, *279*, 14561-14569.
27 Andruniow, T.; Zgierski, M. Z.; Kozlowski, P. M. *J. Phys. Chem. B* **2000**, *104*, 10921-10927.
28 Jensen, K. P.; Sauer, S. P. A.; Liljefors, T.; Norrby, P.-O. *Organometallics* **2001**, *20*, 550-556.
29 Dölker, N.; Maseras, F.; Lledos, A. *J. Phys. Chem. B* **2001**, *105*, 7564.
30 Andruniow, T.; Kozlowski, P. M.; Zgierski, M. Z. *J. Chem. Phys.* **2001**, *115*, 7522-7533.
31 Andruniow, T.; Zgierski, M. Z.; Kozlowski, P. M. *J. Am. Chem. Soc.* **2001**, *123*, 2679-2680.
32 Jensen, K. P.; Ryde, U. *J. Mol. Struct. THEOCHEM* **2002**, *585*, 239-255.
33 Jensen, K. P.; Ryde, U. *J. Am. Chem. Soc.* **2003**, *125*,13970-13971.
34 Jensen, K. P.; Ryde, U. *J. Phys. Chem B.* **2003**, *107*, 7539-7545.
35 Wondimagegn, T.; Ghosh, A. *J. Am. Chem. Soc.* **2000**, *122*, 6375-6381.
36 Ghosh, A.; Wondimagegn, T.; Ryeng, H. *Curr. Opin. Chem. Biol.* **2001**, *5*, 744-750.
37 Pelmenschikov, V .; Blomberg, M. R. A.; Siegbahn, P. E. M.; Crabtree, R. H. *J. Am. Chem. Soc.* **2002**, *124*, 4039-4049.
38 Pelmenschikov, V.; Siegbahn, P. E. M. *J. Biol. Inorg. Chem.* **2003**, *8*, 653-662.
39 Craft, J. L.; Horng, Y. C.; Ragsdale, S. W.; Brunold, T. C. *J. Am. Chem. Soc.* **2004**, *126*, 4068-4069.

metalloenzymes has grown strong and independent today, mainly because of the success of DFT in handling transition-metal complexes.[40]

Methods

Models

We use the full porphine (Por), corrin (Cor), or hydrocorphin (Hcor) ring systems in our models (Figure 2), because loss of equatorial conjugation may have a drastic effect on the electron structure. For Hcor, the two external rings were included as well (Figure 2c). Other ring substituents have been found to have little effect on ground-state structure and properties in both porphyrins[41] and corrins[42] and were therefore ignored. For Hcor, the effect of some of the substituents were studied in more detail (see below).

In addition to the metal ion (M) and the ring system (R), we have added a number of different axial ligands to some complexes, viz. imidazole (Im) as a model of the His or dimethylbenzimidazole ligands in many haem or vitamin B_{12} enzymes, acetamide (Am) as a model of the Gln ligand in MCR, a methyl group (Me), or a hydroxide ion (OH^-), as a model of hydrolysed complexes. Thus, we have studied the following models: four-coordinate complexes without any axial ligands for M^I and M^{II}, five-coordinate complexes with either Im, Am (both M^I and M^{II}), or Me (M^{II}), and six-coordinate complexes with two axial ligands: either Im_2, ImMe, AmMe (M^{II} and M^{III}), ImOH, or AmOH (only M^{III}).

All these combinations of axial ligands have been studied with Cor and Hcor and with Ni and Co in various oxidation and spin states. For all complexes without Im or Am and for the $MRIm_2$ models, we also included Fe and Por in the comparison.

Computational details

All geometry optimisations were performed with the Becke 1988 exchange functional combined with the Perdew 1986 non-local correlation functional (BP86).[43,44] Some energies were also calculated with the B3LYP method[45] (to make them comparable with earlier investigations[16]), which combines some exact Hartree–Fock exchange energy (20%) with the Becke exchange and the local spin-density correlation

40 Siegbahn, P. E. M.; Blomberg, M. R. A. *Annu. Rev. Phys. Chem.* **1999**, 50, 221-249.
41 Sigfridsson, E.; Ryde, U. *J. Biol. Inorg. Chem.* **2003**, *8*, 273-282.
42 Jensen, K. P.; Mikkelsen, K. V. *Inorg. Chim. Acta* **2001**, *323*, 5-15.
43 Becke, A. D. *Phys. Rev. A* **1988**, *38*, 3098-3100.
44 J. P. Perdew, *Phys. Rev. B* **1986**, *33*, 8822.
45 Becke, A. D. *J. Chem. Phys.* **1993**, *98*, 5648-5652.

functional of Vosko–Wilk–Nusair[46] with the non-local Lee–Yang–Parr correlation functionals.[47,48,49] Both BP86 and B3LYP methods incorporate dynamic correlation at a significantly lower cost in terms of cpu-time than perturbation theory, configuration interaction, and coupled-cluster techniques. However, it is important to choose the proper functional for a given task. In general, B3LYP gives best energies among the commonly used density functionals.[50] Yet, we have recently shown that for computing the M–C bond dissociation energies of tetrapyrroles and related systems, BP86 give results close to experiments, whereas the B3LYP energies are ~50 kJ/mole lower.[34] Moreover, BP86 gives more accurate geometries around the metal ions, both for haem and vitamin B_{12} models.[34,51]

The calculations were carried out with the Turbomole program[52], versions 5.5 and 5.6. The basis sets used for geometry optimisation were 6-31G(d) for all atoms, except the metals. For Co, Ni, and Fe, we used the double-ζ basis set of Schäfer *et al*. (contraction scheme $14s11p6d1f$ / $8s7p4d1f$),[53] augmented with two p, one d, and one f functions (with the following exponents: Co: 0.141308, 0.043402, 0.1357, and 1.62; Fe: 0.134915, 0.41843, 0.1244, and 1.339; Ni: 0.146588, 0.044447, 0.1458 and 3.04). Only the pure five d and seven f-type functions were used. Such a basis set has successfully been used before for similar systems and has been shown to give balanced result that are similar to those obtained with larger basis sets.[34,51] We applied the default (m3) grid size of Turbomole, and all optimisations were carried out in redundant internal coordinates. Fully unrestricted calculations were performed for the open-shell systems. We made use of the default convergence criteria, which imply self-consistency down to 10^{-6} Hartree (2.6 J/mole) for the electronic energy and 10^{-3} a.u. for the largest acceptable norm of the gradient.

Solvation energies

Normal quantum chemical calculations are performed in vacuum, whereas the real biological reactions take place in water solution or in proteins. In order to correct for this discrepancy, we have calculated solvation energies for most complexes using the continuum conductor-like screening model (COSMO) [54,55], as implemented in Turbomole. In this method, the solute molecule forms a cavity within a dielectric

46 Vosko, S. H.; Wilk, L.; Nusair, M. *Can. J. Phys.* **1980**, *58*, 1200-1211.
47 Colle, R.; Salvetti, O. *Theor. Chim. Acta.* **1975**, *37*, 329-334.
48 Lee, C.; Yang, W.; Parr, R. G. *Phys. Rev. B.* **1988**, *37*, 785-789.
49 Hertwig, R. H.; Koch, W. *Chem. Phys. Lett.* **1997**, *268*, 345-351.
50 Jensen, F. *Introduction to Computational Chemistry*, John Wiley & Sons, Chichester, **1999**.
51 Ryde U, Nilsson K. *J. Am. Chem. Soc.* 2003; **125**: 14232-14233
52 Alrichs, R.; Bär, M.; Häser, M.; Horn, H.; Kölmel, C. *Chem. Phys. Lett.* **1989**, *162*, 165-169.
53 Schäfer, A.; Horn, H.; Ahlrichs, R. *J. Chem. Phys.* **1992**, *97*, 2571-2577.
54 Klamt, A.; Schüürmann, J. *J. Chem. Soc. Perkin Trans.* **1993**, *2*, 799-805.
55 Schäfer, A.; Klamt, A.; Sattel, D,; Lohrenz, J. C. W.; Eckert, F. *Phys. Chem. Chem. Phys.* **2000**, *2*, 2187-2193.

continuum characterised by a dielectric constant, ε. The charge distribution of the solute polarises the dielectric medium and the response of the medium is described by the generation of screening charges on the surface of the cavity.

These calculations were performed with default values for all parameters (implying a water-like probe molecule) and with a dielectric constant of 80 and 4, to model both pure water and to get a feeling of possible effects in a protein (where the effective dielectric constant is normally estimated to be 2–16 [56,57]). For the generation of the cavity, a set of atomic radii has to be defined. We used the optimised COSMO radii in Turbomole (H: 1.30 Å, C: 2.00 Å, N: 1.83 Å, O: 1.72 Å, Co, Ni, and Fe: 2.00 Å).[58]

Reduction potentials were estimated from these energies in a solvent according to Eqn. 1:

$$E^0 = E(\text{ox}) - E(\text{red}) - 4.43 \text{ eV} \tag{1}$$

where the factor of 4.43 eV represents the potential of the standard hydrogen electrode[59].

Results and Discussion

The model of F430

The full F430 cofactor contains two methyl, an amide, and five carboxylate side chains (see Figure 1). Two of the latter, at positions 12 and 13 have been proposed to interact with the lactone ring, thereby straining the central cavity (cf. Figure 1).[35] The alternative 12,13-diepimer, which forms spontaneously in vitro,[60] gives significantly different structures than F430, when studied by density functional methods.[35] In particular, the ring of the diepimer becomes much more distorted (ruffled) and gives shorter $Ni–N_{eq}$ distances (average 1.97 and 1.93 Å for Ni^I and LS Ni^{II}, compared to 2.04 and 1.97 Å in a F430 model). Therefore, Wondimagegn and Ghosh argued that a proper F430 model must include at least the first carbon atom of all side chains (i.e. eight methyl groups). However, later studies have shown that a model without any side chains gives structures quite close to the methylated F430 model.[35] Such a model was also used

56 Sharp, K. A. *Annu. Rev. Biophys. Biophys. Chem.* **1990**, *19*, 301-332.

57 Honig, B.; Nicholls, A. *Science* **1995**, *268*, 1144-1149.

58 Klamt, A.; Jonas, V.; Bürger, T.; Lohrenz, J. C. W. *J. Phys. Chem. A* **1998**, *102*, 5074-5085.

59 Reiss, H.; Heller, A. *J. Phys. Chem.* **1985**, *89*, 4207-4213.

60 Pfaltz, A.; Jaun, B.; Diekert, G.; Thauer, R. K.; Eschenmoser, A. *Helv. Chim. Acta* **1985**, *68*, 1338-1358.

in other quantum chemical studies of MCR.[37,61]

We have checked the effect of including methyl groups on C12 and C13 (HcorMe$_2$). As can be seen in Table 1, these methyl groups have a minor effect on the structure of four-coordinate Ni^{II} complexes (in the LS state): The Ni–N distances change by at most 0.01 Å for all complexes. Likewise, the difference in the Mulliken charges on the Ni atom is minimal, at most 0.01 e.

However, for the corresponding Ni^I complex, the differences are somewhat larger, viz. up to 0.05 Å and 0.05 e for the spin density on Ni. Yet, this is not an effect of the methyl groups themselves, but it is caused by a change in the conformation of the Hcor ring. As can be seen in Figure 3, the ring is nearly planar in the Ni^{I}HcorMe$_2$ complex (Figure 3c), whereas it is distinctly distorted in the Ni^{I}Hcor complex (Figure 3a). Both conformations can be obtained with the two complexes and they differ by less than 1 kJ/mole. If we compare the geometries of the planar structures of Ni^{I}Hcor (Figure 3b) and Ni^{I}HcorMe$_2$, we see that the differences are as small as for the Ni^{II} complexes (which all are in the distorted configuration).

Thus, we can conclude that the methyl side chains have a very small influence on the geometry and properties of the model. Therefore, we have in the following replaced all side groups on the Hcor ring by hydrogens, in the same way as in the models of Cor and Por. However, the results also show that Hcor can give rise to several different conformations. The same is observed for many of the other complexes also. Therefore, we have thoroughly checked that we always compare complexes with the same conformation.

In Table 1, we also include the 12,13-diepimer of HcorMe$_2$. It can be seen that it gives essentially the same results as the corresponding Hcor model, provided that the configuration of the Hcor ring is the same (both diepimer structures are in the distorted configuration, cf. Figure 3d): The Ni–N distances differ by less than 0.01 Å and the Ni charges and spin densities by less than 0.01 e. This difference is much smaller than reported by Wondimagegn and Ghosh, (up to 0.15 Å).[35] A direct comparison of the results shows that the difference comes mainly from the Ni^{II} state with the F430 model and the Ni^I state of the diepimer: For the former, we obtain ~0.06 Å shorter distances (1.89–1.97 Å) than they do (1.94–2.05 Å; 1.93–2.02 Å with our Hcor model[36]). For the latter the opposite is true; our distances (2.00–2.10 Å) are 0.05–0.11 Å longer than theirs (1.95–1.99 Å). It may also be noted that we get more spin on Ni^I than they did (0.86 compared to 0.56 e). This indicates that the systems are quite flexible so that small

61 Craft, J. L.; Horng, Y. C.; Ragsdale, S. W.; Brunold, T. C. *J. Biol. Inorg. Chem.* **2004**, *9*, 77-89.

differences in the theoretical method give rather large differences in the geometric and electronic structure. This is confirmed in our calculations: structures with distances constrained to those obtained by Wondimagegn and Ghosh are only ~7 kJ/mole less stable than the optimised ones and optimised structures of the same complex started from different conformations may differ by up to 0.05 Å in the Ni–N_{eq} distances, although the energy differs by less than 1 kJ/mole.

It is notable, however, that we obtain the same energy difference between the two epimers: 17 and 20 kJ/mole in favour for the diepimer of Ni^{II} and less than 5 kJ/mole in favour of the diepimer for Ni^{I}. However, it is clear that our results do not support the suggestion that the two epimers have widely different geometries and that this may be a reason why the protein should favour the F430 epimer.[36] On the contrary, the energies involved are too low to be of any physiological importance.

Flexibility of tetrapyrrole rings

One of the most important differences between various ring systems is the inherent size of the central cavity (i.e. what is the ideal size of a metal ion to be bound in the ring) and its flexibility (i.e. how easily can the ring be modified to accommodate ions of other sizes).[62] We have investigated this issue by optimising the geometry of the metal-free, but deprotonated rings with constrained trans N–N distances. In this way, we obtain the optimum cavity size of each ring system and the energy cost to change it. In this study, we also included three other tetrapyrroles (Figure 4), isobacteriochlorin (Ibc), which is saturated at two (vicinal) of the four pyrrole rings (it is a model of sirohaem, which is a precursor in haem synthesis and is employed in some assimilatory NO_2-reducing microorganisms), chlorin fused with an external five-membered lactone (Chl), which has one saturated pyrrole ring (the basic unit of chlorophyll A), and bacteriochlorin fused with an external five-membered lactone (Bchl), which is similar to Chl, but with two saturated (opposite) pyrrole rings. The results are presented in Figure 5.

The Por ring is fully symmetric with two trans N–N distances of 4.17 Å and the Ibc and Cor rings are nearly symmetric. The Ibc ring has a slightly larger cavity size of 4.25 Å, whereas the Cor ring has a much smaller cavity with N–N distances of 3.93 Å. The other three ring systems are inherently unsymmetrical with widely differing trans N–N distances. For Chl, the two N–N distances are 3.99 and 4.35 Å (average 4.17 Å), i.e. similar to that in Por. The cavity of Bchl is slightly larger with N–N distances of 3.98 and 4.42 Å (average 4.20 Å). For Hcor, there are several local minima on the

---

62 Stolzenberg, A. M.; Stershic, M. T. J. Am. Chem. Soc. **1988**, *110*, 6391-6402.

potential surface as can be seen in Figure 5b. There is one with a roughly planar ring and N–N distances of 4.23 and 4.44 Å (average 4.34 Å). However, there is also another form with a severely distorted ring and N–N distances of 4.14 and 4.99 Å (average 4.57 Å). It is actually 41 kJ/mole lower in energy for the isolated monoanionic ring. Thus, the optimum average cavity size follows the trend Cor < Por $\approx$ Chl < Bchl < Ibc < Hcor.

The Por, Ibc, Chl and Bchl rings are also almost equally flexible and give rise to a nearly harmonic potential (compressions and expansions of cavities lead to the same energy penalties; curves around the smaller and larger N–N distances are also identical). In all three cases, a distortion of the central cavity by 0.2 Å costs ~6 kJ/mole, corresponding to a force constant of 155 kJ $mole^{-1} Å^{-2}$ for Chl, 158 kJ/mole/$Å^2$ for Bchl, and 146 kJ/mole/$Å^2$ for Por and Ibc. This is smaller than a force constant for a covalent bond (1000–2400 kJ/mole/$Å^2$), but similar to that of metal–ligand bonds (40–500 kJ/mole/$Å^2$).[63] It shows that ions of quite different sizes may fit into the ring at a rather small expense in energy. The Cor ring is more flexible, with a force constant of only 48 kJ/mole/$Å^2$ and a penalty of 2 kJ/mole for a 0.2 Å distortion. Owing to the widely different bond lengths and the multiple minima (Figure 5b), the N–N distance in Hcor can be varied over 1.6 Å (3.8–5.4 Å) at an expense in energy of less than 10 kJ/mole. Thus, the flexibility of the rings follows the trend Hcor > Cor > Por $\approx$ Ibc > Chl > Bchl. This is in good accordance with previous suggestions that the Hcor ring should be more flexible than Por, but it clearly shows that Cor is not more rigid than Por, contrary to what was suggested before.[62]

Spin states

Transition metals with open $3d$ orbitals can attain several spin states with different geometries, but often with similar energies. Thus, the d^5 and d^6 ions (Fe^{III}, Fe^{II}, and Co^{III}) can attain three spin states, high spin (HS), intermediate spin (IS), and low spin (LS) depending on whether zero, one, or two $3d$ orbitals are unoccupied. Likewise, the d^7 and d^8 ions (Fe^{I}, Co^{II}, Ni^{III}; Co^{I} and Ni^{II}) can attain two spin states, HS and LS, whereas the d^9 ion Ni^{I} can only attain one spin state. We have studied the relative energies of the various spin states for most of the complexes and metals, in order to decide the ground state of the various complexes. The results are collected in Table 2.

It can be seen that Co in all three oxidation states and ring systems consistently prefers the LS state by 6–166 kJ/mole. For iron, the results are also quite straightforward (at least for the relatively few complexes in this investigation): four-

---

63 De Kerpel, J. O. A.; Ryde, U. *Proteins* **1999**, *36*, 157-174.

coordinate Fe^{II} is IS, in accordance with experiments,[64,65] whereas the other complexes (four-coordinate Fe^{I}, six-coordinate Fe^{II} and Fe^{III} with Im_2, and five-coordinate Fe^{II} with OH or Me) all are LS (by 52–260 kJ/mole).

Ni^{I} has only one spin state and does not need to be discussed further. For Ni^{III}, the BP86 calculations indicate that the LS state is 19–182 kJ/mole more stable than the HS state (which contain 0.7–1.3 unpaired electrons in the ring system and therefore is HS Ni^{II} coupled to a ring radical). However, B3LYP energies for the $Ni^{III}RIm_2$ complexes are quite different and favour the HS state by 54–60 kJ/mole more than the BP86 method. Therefore, B3LYP actually predicts a HS ground state for $Ni^{III}PorIm_2$ and $Ni^{III}HcorIm_2$ (but still as Ni^{II} and a ring radical).

It is a well-known problem that various DFT functionals give widely different spin splitting energies.[66] In fact, the problem seems to be related to the amount of exact (Hartree–Fock) exchange in the functional: Pure functionals (i.e. without any exact exchange), like BP86, in general favour LS states, whereas hybrid functionals (like B3LYP) favour HS states. Attempts have been made to calibrate the functionals to better reproduce spin-splitting energies of transition-metal complexes (Fe–S complexes) and it has been suggested that the best results are obtained with about 16% exact exchange in the functional (rather than the 20% present in B3LYP).[66] However, for blue-copper protein models, 38% exact exchange gave better results for spin densities and spectroscopic properties, indicating that the result is not general.[67] Therefore, it is not fully clear which state is most stable for the Ni^{III} complexes, although previous investigations have assumed the LS state.[36,37,38] We will follow this custom.

For Ni^{II}, the results are even harder to interpret because the LS and HS states have different coordination preferences: The LS state has a doubly occupied d_{z^2} orbital and an empty $d_{x^2-y^2}$ orbital. Therefore, it is Jahn–Teller unstable and will prefer a square-planar geometry with weakly bound axial ligands, which often dissociate from the metal and forms a hydrogen bond to another part of the complex. In the HS state, on the other hand, both the d_{z^2} and $d_{x^2-y^2}$ orbitals are singly occupied, leading to a preference of tetrahedral or octahedral structures, and in our models to a higher affinity for the axial ligand. Consequently, the LS and HS energies for the Ni^{II} complexes with a weak axial ligand (Im and especially Am) are often not comparable, because the energy of the dissociated axial ligand is not well-defined (it forms hydrogen bonds to different atoms

64 Goff, H.; La Mar, G. N.; Reed, C. A. *J. Am. Chem. Soc.* **1977**, *99*, 3641-3646.
65 Kitagawa, T.; Teraoka, J. *Chem. Phys. Lett.* **1979**, *63*, 443-446.
66 Reiher, M.; Salomon, O.; Hess, B. A. *Theor. Chem. Acc.* **2001**, *107*, 48-55.
67 Solomon, E. I.; Szilagy, R.K.; DeBeer George, S.; Basumallick, L. *Chem. Rev.* **2004**, *104*, 419-458.

on the periphery of the complex). On the other hand, this also means that a protein may stabilise the HS states by providing an axial ligand. This may be the role of the Gln residue found in MCR.

This is supported by the results in Table 2: The four-coordinate (square planar) Ni^{II} complexes have a LS ground state (by 100–157 kJ/mole), whereas the five-coordinate complexes with the strong methyl or OH^- ligands are HS by 13–86 kJ/mole. Interestingly, the LS state of these complexes also binds the axial ligand, but in these cases, the electronic structure changes so that the $d_{x^2-y^2}$ orbital becomes occupied, leading to a increase in some of the equatorial Ni–N distances. For the $Ni^{II}RIm$, $Ni^{II}RAm$, and $Ni^{II}RIm_2$ complexes, the Im or Am ligands of the LS states have dissociated (marked by bold face in Table 2), whereas the ligands remain bound to the metal ion in almost all HS states. The LS states have a 18–106 kJ/mole lower energy, but this only reflects that the hydrogen bond of the Im or Am ligand to the periphery of the molecule is more favourable than the bond to the metal. If the axial ligand is forced to bind also in the LS state, the energy difference is reduced by 34–73 kJ/mole so that the two spin states become quite close in energy (the HS state is actually lowest for $Ni^{II}HcorIm$). Moreover, we have the same tendency of BP86 to overstabilise the LS state by 44–60 kJ/mole compared to the B3LYP method as for Ni^{III}. Finally, the Im and Am ligands dissociates also in the HS state of the $Ni^{II}HcorImMe$ and $Ni^{II}RAmMe$ complexes.

We decided to consider the HS as the ground states of all the five- and six-coordinate Ni^{II} complexes because we want to study the effect of the axial ligands. This spin state has also been used in previous studies of coenzyme F430.[36,37] For the three complexes where the axial ligand dissociates also in the HS state, we fixed this distance to reasonable values (cf. Table 2).

In the following, we will restrict the discussion to the most stable spin states, if not otherwise stated. For complexes with Im and Am ligands, we will also require that the axial ligand remains bound in all states considered. Thus, for Ni^{III}, the LS state will be discussed, whereas for Ni^{II}, the LS state will be used for four-coordinate complexes, whereas the HS state will be used for five- and six-coordinate complexes.

Thermodynamic stability of metal and ring combinations

From a purely thermodynamic perspective, nature might have chosen some combinations of metals and tetrapyrroles on grounds of stability. There are nine possible combinations of ring systems and monovalent metal ions. These nine possibilities can

be assigned a relative stability by considering metal-substitution reactions of the form

$$M_iR_j + M_jR_i \rightarrow M_jR_j + M_iR_i \tag{2}$$

where M_i, M_j = Co, Fe, or Ni, and R_i, R_j = Cor, Por, or Hcor. Such reactions have a large information content owing to the cancellation of errors in the scheme: All bond types are the same on both sides of the reaction arrow (an isodesmic reaction) and the correlation and vibrational energies are expected to be similar. The nine possible reaction energies for metal substitution of the four-coordinate M^IR complexes, Eqn. 2, are presented in Table 3, calculated in vacuum ($\varepsilon = 1$), a protein-like solvent ($\varepsilon = 4$), and aqueous solution ($\varepsilon = 80$). The effect of solvation is quite restricted, <19 kJ/mole, as might be expected for these reactions that have almost identical charge densities and solvent-accessible surfaces. The trends are general, so we will only discuss vacuum energies in the following.

Reaction number 1, 5, and 9 are substitution reactions where two native forms (FePor, NiHcor, and CoCor) interchange metals. A striking observation is that all three native forms are favoured in the three substitution reactions, by 13–50 kJ/mole. We can conclude that the intrinsic energies of the metal complexes favour the native combinations. These energies also indicate that FePor is the least stable of these native combinations, because the formation of FePor is endothermic in reaction 4, at least in solution.

Similar reactions can be formed for all the other complexes investigated. The four complexes we have studied for all nine combinations of rings and metals ($M^{II}R$, $M^{II}RMe$, $M^{II}RIm_2$ and $M^{III}RIm_2$) are also included in Table 3 (only vacuum values). It can be seen that all four give similar results to that of M^IR, i.e. they are also favourable for the native combinations, except for reaction 1 with the $M^{II}RMe$ model and reaction 9 with the $M^{II}R$ model, for which the reaction energies are unfavourable by 4–7 kJ/mole.

For the complexes we have only studied for Co and Ni, we give in Table 4 the corresponding energies for reaction 9, i.e.

$$NiCorXY + CoHcorXY \rightarrow CoCorXY + NiHcorXY \tag{3}$$

for any axial ligands X and Y. Again, the results show that the native CoCor and NiHcor combinations are stabilised for all complexes in the investigation (by 6–93 kJ/mole), except for the $M^{II}R$ model mentioned above. Thus, the metal ions have undoubtedly

been selected to preferentially fit into their native ring system. In the following, we will try to understand why, and we will also study the functional effects of this selection.

Electronic structure of the $M^I R$ complexes

The spin densities of the four-coordinate $M^I R$ complexes are presented in Table 5. It can be seen that the $Ni^I Cor$ complexes exhibits significant spin in the ring system (0.8 e in Cor and 0.2 e on Ni). Thus, this complex contains to a large extent IS Ni^{II} antiferromagnetically coupled to a ring radical. On the other hand, the $Ni^I Por$ and $Ni^I Hcor$ complexes are almost pure Ni^I. This is in accordance with earlier calculations on $Ni^I Hcor$[35] and experiments.[68,69]

The highest occupied molecular orbital (HOMO) energies in Table 6 give an impression of the electronic stability of the systems and their ability to give away electrons. The most important observation is that porphine HOMOs are high in energy, owing to the large inter-electronic repulsion in the anionic complexes; in fact, they are all positive. However, it also varies with the nature of the metal: FePor and CoPor have similar E_{HOMO} of ~0.2 eV, whereas that of NiPor is higher (+0.70). This trend, Fe ≈ Co < Ni, holds true for the other two rings as well: Thus, in all complexes, Ni is the more nucleophilic, and it is easier to promote an electron to the lowest unoccupied molecular orbital (LUMO), in so far as the gap energy has physical significance. The results quantify that porphyrins are not suitable to stabilise the reduced M^I states. If a protein wants to gain access to the monovalent metal state, it has to use Cor or Hcor. Moreover, the results show that Ni^I is predicted to be more nucleophilic than the "supernucleophile" Co^I.

Equatorial $M-N_{eq}$ distances, ion sizes, and ring strain

The optimised equatorial metal–nitrogen ($M-N_{eq}$) distances of the fully optimised four-coordinate $M^I R$ models are given in Table 7, together with the distance of the metal ions out of the average N_{eq} plane. For the corrins, we also report the fold angle, which is defined by the angle between two planes going through each half of the corrin ring along the C_2 axis.[70]

The Por complexes are planar with the metal in the ring plane for all metals and spin states. However, the Cor and Hcor complexes are non-planar with the metal ion above the average ring plane by 0.07–0.10 Å for Cor and 0.18–0.27 Å for Hcor.

68 Lexa, D.; Momenteau, M.; Mispelter, J.; Savéant, J.-M. *Inorg. Chem.* **1989**, *28*, 30-35.
69 Pfaltz, A. In: *The Bioinorganic Chemistry of Nickel*, VCH Publishers, **1988**, Chapter 12.
70 A rigirous definition can be found in Ref. 2.

Consequently, all four M–N$_{eq}$ distances are nearly equal in Por, whereas those in Cor come in two sets, which differ by ~0.06 Å (owing to the approximate C_2 symmetry of the Cor ring), and those of Hcor are more varying and differ by 0.04–0.09 Å.

From Table 7, it can be seen that Co always has the shortest average M–N$_{eq}$ bond lengths, whereas those of Fe is 0.02–0.04 Å longer and those of Ni are 0.03–0.12 Å longer (most in Hcor; the bond in Ni^{I}Cor is unusually short, owing to its differing electronic structure). This reflects the ionic radii of the M^I metal ions.

For the M^{II} states, the following can be deduced for the average M–N$_{eq}$ bonds (Tables 8 and 9): LS Ni^{II} < LS Co^{II} < IS Fe^{II} for the four-coordinate complexes and LS Fe^{II} ≈ LS Co^{II} < HS Ni^{II} for the other complexes. However, all differences are small except that HS Ni^{II} gives 0.05–0.12 Å longer bonds than the other ions. The latter results are in qualitative agreement with the ionic radii of octahedral LS Fe^{II}, LS Co^{II}, and HS Ni^{II}, 0.61, 0.65, and 0.69 Å, respectively.[71] For the trivalent states, LS Co^{III} ≈ LS Fe^{III} have the same bond lengths within 0.01 Å. LS Ni^{III} also have a similar bond length in most complexes, but in some of the Me and OH$^-$ complexes it may have up to 0.10 Å longer bonds. This is in accordance with the ionic radii of the octahedral LS metal ions: 0.55, 0.55, and 0.56 Å for Fe^{III}, Co^{III}, and Ni^{III}, respectively.[71]

Thus, the metals give quite similar bond lengths in all complexes, which indicates that there is appreciable strain in the rings. This is confirmed if we compare the various ring systems: the trends are almost independent on the metal ion. Cor gives the shortest M–N$_{eq}$ bond lengths, whereas those in Por are 0.08–0.11 Å longer and those in Hcor are 0.05–0.18 Å longer. This is in accordance with half of the difference in the optimal cavity size for Por and Cor (0.12 Å), but it is smaller than the difference between Cor and Hcor. Taking all complexes together, Por shows a range for the M–N$_{eq}$ distances of 0.10 Å (1.97–2.07 Å), Cor 0.11 Å (1.87–1.98 Å), and Hcor 0.18 Å (1.92–2.10 Å). This reflects the intrinsic flexibility of the ring systems.

It is notable that for all ring systems, there are a few complexes with strong axial ligands (OH or Me) that have one very large M–N$_{eq}$ distance (up to 2.10 Å in Cor and 2.78 Å in Hcor), reflecting that the unoccupied orbital has changed from $3d_{z^2}$ to $3d_{x^2-y^2}$. This explains the atypical average Co–N$_{eq}$ distances of Co^{II}HcorMeIm and Co^{II}HcorMeAm.

In order to obtain an estimate of the intrinsic M–N$_{eq}$ bond lengths and the strain in the ring systems, we have cut the three ring systems into non-cyclic counterparts (two NH(CH)$_3$NH$^-$ halves for Por, called PMod in the following, (CH$_2$N(CH$_2$)$_2$NCH$_2$)

---

71 Holm, R. H.; Kennepohl, P.; Solomon, E. I. *Chem Rev.* **1996**, *96*, 2239-2314.

$(NH(CH)_3NH)^- = CMod$ for Cor, and $CH_2N(CH_2)_2CHNH)(NH(CH)_3NH)^- = HMod$ for Hcor; cf. Figure 6) as has been done before for Por and Cor.[16,20] Such models retains the number of carbon atoms in the chelate ring and the total charge and hybridisation of the ring system, but it removes restraint on the metal–ligand distances imposed by the closed ring system. The optimised bond lengths of the $M^{I/II}$ and $M^{II/III}Im_2$ complexes are presented and compared to those obtained with the full ring systems in Table 8.

The results show that the central cavity of Por is too large (by 0.08–0.15 Å) for all three metals, except for HS Ni^{II}. This is the reason why mixed-spin chemistry is observed in haem biochemistry[16], because the large cavity gives access to the higher spin states. Likewise, the cavity size of Cor seems to be ideal (within ± 0.02 Å) for all metals except HS Ni^{II} and Ni^{III}. This was also observed in our previous investigation of Co and Fe.[16]

HMod is similar to CMod but it does not contain the missing methine link in Cor. They are both worse than PMod because they involve one charged and one uncharged moiety, and also because they are somewhat more sterically crowded. As a result of the crowding, all complexes with this ligand are non-planar. Consequently, the $M–N_{eq}$ bond lengths differ quite extensively (by 0.01–0.15 Å). In Table 8, only the average distances are given. However, they give almost the same average $M–N_{eq}$ bond lengths, with Ni^I as the only slight exception (Table 8) . It can be seen that HMod gives 0.04–0.09 Å shorter distances than Hcor, indicating that the cavity size in Hcor is too large for all metals, again except for HS Ni^{II}. Thus, Hcor seems to be designed to allow for the large HS Ni^{II} ion . On the other hand, our results do not support the suggestion that Hcor should be designed to fit the large Ni^I ion:[35,36] The average $Ni^I–N_{eq}$ bond length is 0.09 Å shorter in HMod than in Hcor.

Me and OH ligands

We now turn from the equatorial to the axial ligands and look on the strong, negatively charged Me^- and OH^- ligands. The M–Me and M–OH bond distances in the various complexes are shown in Table 10. It can be seen that the M–Me distances are in general 1.94–1.99 Å, quite independent of the metal and ring system, except that Fe has ~0.04 Å longer bonds than the other two metals. However, for six complexes, the distance is appreciably longer, 2.05–2.10 Å (these complexes are marked in bold face in Table 10). This is related to a change in the electronic structure of the complex, as can be seen in Table 11: Complexes with a short M–Me bond have a small spin on the methyl group (<0.1 e), indicating a pure CH_3^- group, whereas those with a long bond

have a significant spin on the methyl group, 0.2–0.4 *e* (marked in bold face also in Table 11), indicating that it has a significant CH$_3$• radical character, which explains the long bond. We have tried to find the corresponding state with a short M–Me bond for these complexes by constrained optimisations, but these states have turned out to be ~5 kJ/mole less stable. Apparently, these two states are so close in energy that their relative stability may change by small changes in the model or in the surroundings.

The spin densities in Table 11 also show that the Co^{II} Por and Co^{II}Cor complexes fall out by having essentially no charge on the metal ion (<0.05 *e*), but instead all the spin in the ring. Thus, these complexes are in practice a methyl radical bound to Co^{I}.

The OH complexes behave analogously: Half of the complexes (those with closed-shell the metals Fe^{II} and Co^{III}, and Ni^{III}HcorOHIm) give M–OH bonds of 1.85–1.90 Å, whereas the other complexes have longer M–OH bonds (1.96–2.05 Å; marked in bold face in Table 10). Again, the longer distances are connected with a partial radical character of the OH group (0.2–0.4 *e* spin density; cf. Table 11) and the two states are close in energy (~10 kJ/mole). In the following, we will only discuss the most stable states, i.e. those shown in Table 10.

The importance of the weak trans axial ligand (Im or Am)

The importance of axial ligands in biological cofactors has been much discussed and they are considered to modulate the reactivity of the cofactor: For haem proteins, the proximal ligand has been proposed to induce a trans electronic effect, often called the "push" effect.[72] When the proximal ligand is His, it directly influences the electronic structure at the iron site and can tune it by hydrogen bonds.[25] In cobalamins, a trans-steric effect of His or 5,6-dimethylbenzimidazole (DMB) has been proposed to deform the tetrapyrrole ring and induce a weakening of the Co–C bond.[73,74] However, this mechanism has not gained any theoretical support.[29,31,32] The X-ray structure of MCR indicates that the Ni^{II} state has an axial ligand bound in the form of Gln-147[5,75] and it has been suggested that this ligand may activate Ni^{I} towards nucleophilic attack.[76] In addition, it has been shown to change the preferred spin state of Ni^{II} from LS to HS.[77] EXAFS data indicates that it binds also in the Ni^{I} state.[13]

M–Im and M–Am distances of our optimised complexes are listed in Table 12. It

72 Dawson, J. H. *Science* **1988**, *240*, 433-439.
73 Firth, R. A.; Hill, H. A. O.; Pratt, J. M.; Thorp, R. G.; Williams, R. J. *J. Chem. Soc. A* **1968**, *10*, 2428.
74 Grate, J. H.; Schrauzer, G. N. *J. Am. Chem. Soc.* **1979**, *101*, 4601-4611.
75 Shima,S.; Goubeaud, M.; Vinzenz, D.; Thauer, R. K.; Ermler, U. *J. Biochem*. **1997**, *121*, 829-830.
76 Ermler, U.; Grabarse, W.; Shima, S.; Goubeaud, M.; Thauer, R. K. *Curr. Opin. Struct. Biol.* **1998**, *8*,749-758.
77 Renner, M. W.; Fajer, J. *J. Biol. Inorg. Chem.* **2001**, *6*, 823-830.

can be seen that in the five-coordinate complexes, Ni^{II} gives appreciably shorter Me–Im (~0.1 Å) and Me–Am (0.15–0.27 Å) bonds than does Co^{II}. However, in the complexes with Me and OH, the difference is smaller: The M–Im distance is 2.11–2.19 Å in all $M^{II/III}RMeIm$ complexes and 2.01–2.03 Å in the $M^{III}ROHIm$ complexes. The corresponding values for the M–Am distances are 2.17–2.37 Å and 2.07–2.10 Å. However, three $M^{III}ROHIm/Am$ complexes have much longer M–Im/Am distances (2.49–2.99 Å, but still with the ligand mainly interacting with the metal; they are marked in bold face in Table 12). These are exactly the three complexes that have a long M–OH distance, as discussed in the previous section, showing that this change in the electronic structure also affects the trans axial ligand.

The binding energies of the axial Im and Am ligands in Table 13 show that there is a conspicuous difference between Ni^{II} and Co^{II}: Co^{II} shows a favourable binding of both Im and Am to the four-coordinate $M^{II}R$ complex, by 40–85 kJ/mole for Im and 35–72 kJ/mole for Am. On the other hand, the Im and Am affinities to $Ni^{II}R$ are lower, being strongly unfavourable to the $Ni^{II}Cor$ complex (58–101 kJ/mole), but slightly favourable to the $Ni^{II}Hcor$ complex (by –6 to 44 kJ/mole). The Ni^{II} energies are affected by the change in spin state between the five- and four-coordinate complexes and are therefore less accurate. The binding of Im is 5–17 kJ/mole more favourable than that of Am. Solvation effects are always unfavourable for the binding.

As could be expected, the binding of Im and Am to the $Co^{II}RMe$ complexes is weaker, by ~60 kJ/mole. However, for the $Ni^{II}HcorMe$ complexes, the difference is small and for the $Ni^{II}Cor$ complexes, the binding is actually stronger. This reflects a change in the electronic structure of the Ni^{II} complexes when the strong Me^- ligand is bound, which makes the binding of the weaker axial ligands more favourable. These binding energies are affected by the differing electronic structures of the Me complexes with long and short bonds, the fixing of three M–Im/Am distances, and the long $Co–N_{eq}$ bonds in two complexes, and the energies are therefore somewhat erratic. The binding affinity of a second Im ligand to the $M^{II}RIm$ complexes is always favourable and quite similar for all four systems, 34-66 kJ/mole.

In crystal structures of MCR, a Gln ligand binds to Ni (with a six-coordinate HS Ni^{II} ion bound to the sulphur atom of coenzyme M) with an average distance of 2.29 Å (also the distance in the most accurate structure[78]). There has been some discussion whether the Gln residue is actually bound or is just forced into the vicinity of the metal

78 Grabarse, W.; Shima, S.; Mahlert, F.; Duin, E. C.; Thauer, R. K.; Ermler, U. in: Messerschmidt, A.; Hube, R.; Poulos, T.; Wieghart K. (eds.) *Handbook of Metalloproteins*, John Wiley & Sons, Chichester, **2001**, 897-914.

by the protein backbone.[5] Our calculations show that 2.3 Å is a typical Ni^{II}–Am distance in the six-coordinate HS state. We have also optimised a number of structures with M^I and Im or Am, but in all these structures, the axial ligand dissociated from the metal. However, structures with the Am ligand bound at a distance of ~2.3 Å have essentially the same energy as the dissociated state (within 5 kJ/mole) showing that the binding of this ligand can easily be stabilised by the surrounding protein, as is also observed experimentally.[13] This indicates that Gln is weakly bound to the complex and is used to stabilise the Ni^{II} and Ni^{III} oxidation states.[79] In fact, Gln is probably employed as an ideal weak and flexible ligand, that coordinates the metal when needed. In that way, it is similar to the weak Gln or Met ligands in blue copper proteins.[80]

Homolytic M–C BDEs

After looking at these basic properties of the rings and metal ions, we now turn to some of the typical reactions the tetrapyrroles may have in vivo. We start to look at the strength of a M–Me bond, because both coenzymes B_{12} and F430 have been suggested to be involved in the transfer of an alkyl group. In the first case, alkyl complexes like methyl- and adenosylcobalamin (with Co^{III}) are stable compounds that have been characterised structurally.[81][82]

For the latter, both Ni^{II} and Ni^{III} complexes with a methyl group have been suggested to be involved in the reaction mechanism of MCR: In one of the most widely cited mechanisms of this enzyme,[14] it is suggested that methyl-coenzyme M donates its methyl group to Ni^I in coenzyme F430, giving rise to a Ni^{III}Me complex. In the next step, coenzyme M is oxidised by Ni^{III} to a thiyl radial, giving rise to a Ni^{II}Me complex. The latter is then protonolysed using the proton on the thiyl radical, giving Ni^{II} and a free methane molecule. The thiyl radical reacts with coenzyme B, forming a disulphide radical, which is finally oxidised by coenzyme F430, giving rise to the coenzymes M and B heterodisulphide and the Ni^I state of coenzyme F430. It is possible that the methyl transfer reaction may be coupled to the first redox reaction, so that a Ni^{II}Me complex is formed directly. It is also conceivable that protonolysis takes place directly for the Ni^{III}Me complex. Therefore, these types of reactions will also be studied.

We start by calculating the homolytic bond dissociation energies (BDEs) of the M^{II}–C bond in the five-coordinate M^{II}RMe complex, i.e. the energy of the reaction

79 Yerushalmi, R.; Noy, D.; Baldridge, K. K.; Scherz, A. *J. Am. Chem. Soc.* **2002**, *124*, 8406-8415.
80 Olsson, M. H. M.; Ryde, U.; Roos, B. O. *Prot. Sci.* **1998**, *7*, 2659-2668.
81 Lenhert, P. G. *Proc. R. Soc. Lond. Ser. A.* **1968**, *303*, 45-50.
82 Savage, H.; Lindley, P.; Finney, J.; Timmins, P. *Acta Crystallogr.* **1987**, *B43*, 280-295.

$$M^{II}RMe \rightarrow M^{I}R + Me^{\bullet} \qquad\qquad (4)$$

The calculated M–C BDEs for this reaction are shown in Table 14. It can be seen that they in general follow the trend Fe > Co > Ni, except for in Hcor, where the BDE of Ni is similar to that of Co. The high BDEs of Fe (154–171 kJ/mole) make Fe unsuitable for reversible alkyl transfer. Solvation effects are rather small (6–15 kJ/mole, except for CoPor) and tend to decrease the BDE. It is notable that the coenzyme F430 model has a slightly larger M^{II}–C BDE (73–81 kJ/mole) than that of the coenzyme B_{12} model (61–76 kJ/mole).

We have also investigated the same reaction starting from the M^{III} state. Since the latter state is expected to be six-coordinate, axial ligands were included in the reaction:

$$M^{III}RMeIm/Am^{+} \rightarrow M^{II}RIm/Am^{+\bullet} + Me^{\bullet} \qquad\qquad (5)$$

This is the homolytic (radical generating) M–Me bond dissociation reaction, employed by the adenosylcobalamin proteins. Therefore, it has been studied by several groups for the CoCorIm complex.[16,27,29,31,32,34]

From the results in Table 15, it can be seen that the coenzyme B_{12} model, $Co^{III}CorMeIm^{+}$, has a bond strength of 152–156 kJ/mole, which is very close to the experimental value of 155 ± 13 kJ/mole for methylcobalamin.[83] The BDE is slightly higher in the Hcor ring, ~166 kJ/mole, so the ring system has some effect on this energy. A change of the axial ligand from Im to Am also has a small effect on the BDE (<17 kJ/mole), so these results indicate that the BDE for Co^{III} is quite indifferent both to the ring system and the axial ligand.

However, if the metal is changed, a larger effect is seen: Ni^{III} has 23–43 kJ/mole lower BDEs than Co^{III}. Thus the M–CH_3 bond is appreciably weaker for Ni than for Co. This effect is somewhat reinforced by the shift of the axial ligand and ring system, so our calculations indicate that the F430 model would have ~30 kJ/mole lower BDE than coenzyme B_{12}.

These estimates of the $M^{II/III}$–C BDE can be used to judge the feasibility of various suggested reaction mechanisms of MCR. In the most widely accepted mechanisms,[14] it is suggested that coenzyme M donates the methyl group to Ni^{I}-F430, forming either a sulphur radical (homolytic reaction) or a thiolate (heterolytic reaction, studied in the

---

83 Martin, B. D. ; Finke, R. G. *J. Am. Chem. Soc.* **1990**, *112*, 2419-2420.

next section). Thus, we should compare the results in Table 15 with the energy of the reaction

$$\text{MeSMe} \rightarrow \text{MeS}^{\bullet} + \text{Me}^{\bullet} \qquad\qquad\qquad (6)$$

a simple model reaction of the homolytic dissociation of coenzyme M (previous studies[37] have shown that the reaction energy is insensitive to the actual model of coenzyme M). This reaction is strongly endothermic, giving energies of 315–317 kJ/mole (in water and a vacuum; previous studies[37] gave slightly smaller value, 293 kJ/mole). This shows that it is unlikely that coenzyme M may donate a methyl group to Ni^{I} or Ni^{II}: The coupled reaction would be endothermic by 236–242 kJ/mole for the $\text{Ni}^{\text{I/II}}$ reaction and 190–196 kJ/mole for the $\text{Ni}^{\text{II/III}}$ reaction. The same applies for all metals and ring system studied (the least endothermic reaction energy, 146 kJ/mole is obtained for $\text{Fe}^{\text{I/II}}\text{Cor}$).

Consequently, we can conclude that it is highly unlikely that coenzyme F430 acts as a methyl acceptor in a homolytic reaction in MCR. These results agree with those previously obtained by Pelmenschikov et al.[37] However, they used the B3LYP method, which we have shown to underestimate the BDE.[34] Therefore, it could be expected that we would obtain a less endothermic energy for electron transfer, especially as we also include a model of the axial Gln ligand in MCR. Yet, the energy difference in our obtained BDEs, 7 kJ/mole for $\text{Ni}^{\text{I/II}}$ and 52 kJ/mole for $\text{Ni}^{\text{II/III}}$ is not enough to make the methyl transfer reaction possible.

Heterolytic BDE

Since it is unlikely that coenzyme F430 accepts the methyl group in a homolytic reaction, we tested if a heterolytic reaction is possible instead. This is the reaction assumed to take place in methionine synthase (MS), where homocysteine takes up a methyl group from $\text{Co}^{\text{III}}\text{CorMeIm}$. The reverse of this reaction is putative first step of MCR, where coenzyme M donates its methyl group to $\text{M}^{\text{I}}\text{R}$. Thus, both reactions involves a donor/acceptor that can bind a (formal) methyl cation. We will model it as a CH_3S^- group, because homocysteine in MS is suggested to be deprotonated by binding to a Zn^{2+} ion.[33,84] In MCR, coenzyme M is assumed to immediately take up a proton from coenzyme B, but we assume that this takes place in a separate reaction (to make

84 Peariso, K.; Goulding, C. W.; Huang, S.; Matthews, R. G.; Penner-Hahn, J. E. *J. Am. Chem. Soc.* **1998**, *120*, 8410-8416.

the reactions comparable). Moreover, the donor and acceptor only provide a constant factor in the reaction, irrespectively of their actual identity.

Thus, we will study the reaction:

$$M^{III}RLMe^+ + MeS^- \rightarrow M^IR + L + MeSMe \qquad (7)$$

We have assumed that the axial ligand dissociates in the reaction, as is observed in MS, as well as in our geometry optimisations of the M^I states. It can be seen that the reaction involves the conversion of two oppositely charged complexes to neutral products. Therefore, solvation effects are very important in this reaction, as can be seen in Table 16: The reaction energy decreases from –430 to –515 kJ/mole in vacuum to –51 to –143 kJ/mole in water. However, the relative energies are quite stable. Thus, the reaction energy is more negative for Ni than for Co by 50–80 kJ/mole, indicating the the the M^{III}–Me bond is stronger for Co or that the M^I complex is more stable for Ni. Likewise, the energy is 9–33 kJ/mole lower for Am than for Im in all complexes, confirming that Im binds slightly stronger than Am to M^{III}, thereby stabilising this state. There is no clear difference between Cor and Hcor.

Altogether, we see a 74–85 kJ/mole higher BDE for the coenzyme B_{12} model than for the F430 model. This is a large difference, which shows that NiHcor is an appreciably worse methyl acceptor than CoCor. Moreover, the actual MCR reaction is the reverse of Eqn. 7 and therefore endothermic by 116 kJ/mole in water and by 239 kJ/mole in a "protein-like" environment with a dielectric constant of 4.

However, the reverse reaction is endothermic (by 60–430 kJ/mole) also for the coenzyme B_{12} model, although it is known that this reaction actually takes place in MS. The reason for this is that the protein employs a different donor in this step, viz. methyltetrahydrofolate, which furthermore is believed to be protonated. This choice is essential for the reaction: If we replace the MeS^-/MeSMe donor/acceptor in Eqn. 7 by a realistic model of tetrahydrofolate, then the reaction becomes exothermic for the B_{12} model by 26–107 kJ/mole, whereas the reaction for the F430 model is still endothermic, except in a vacuum (by –21 to 49 kJ/mole; note that the difference between the two models is the same as for the MeS^-/MeSMe pair).

This shows that it is mainly the donor that is the problem in the MCR reaction. It is possible that MCR may employ this heterolytic reaction with a more appropriate donor or by tuning the reactivity of the donor. For example, if coenzyme M is protonated before the methyl transfer, the reaction is readily exothermic (by 35–182

23

kJ/mole) also with the coenzyme F430 model. The same applies for SMe_3^+ as a model of *S*-adenosinemethionine, widely used in biochemistry as a methyl donor. This clearly shows that the primary problem in the suggested reaction mechanisms of MCR lies in the donor of the methyl group, rather than in coenzyme F430: Methyl coenzyme M needs to be activated before it may donate its methyl group to coenzyme F430, just as for all other methyl transfer reactions in biology. Thus, we can conclude that it is too early to dismiss the possibility of Ni–methyl intermediates in the reaction mechanism of MCR.

Protonolysis and hydrolysis

In the reaction mechanism of MCR, discussed above, the Ni^{II}–C bond is protonolysed by a proton taken from coenzyme M. Our data allows us to study also this reaction. We will assume that the proton comes from MeSH, giving a free MeS^- anion after the reaction:

$$M^{II}RMeIm/Am + MeSH \rightarrow M^{II}RIm/Am^+ + CH_4 + MeS^- \tag{8}$$
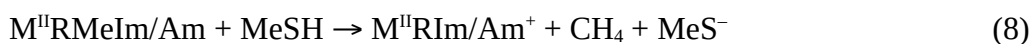
It should be noted, however, that the relative energies for the various metals or ring systems are completely independent of the proton donor. We have studied this reaction for complexes both without and with an axial ligand (Im or Am). The results are collected in Table 14.

It can be seen that the reaction energy depends strongly on the solvation, as can be expected for a proton-transfer reaction, where two oppositely charged molecules are formed from neutral reactants. This also means that the Por ring, with its double negative charge gives a more exothermic result than the other two rings (by 331–371 kJ/mole in vacuum). However, there is also pronounced differences between the three metals: Fe has the most endothermic energies, whereas Ni has the most exothermic energies (the Fe–Ni and Co–Ni differences are 101–208 and 50–134 kJ/mole, respectively).

Axial ligands have a pronounced effect on these energies, increasing the endothermicity with the strength of the ligand, at least for the Co complexes (the results of the Ni complexes are different owing to that most of these complexes have a different electronic state with significant spin density on the methyl group, cf. Table 11). As a result, the protonolysis energy of the F430 model is actually 12–23 kJ/mole less exothermic than that of the B_{12} model. Thus, we see no pronounced enhancement of the

protonolysis reaction for F430. It is notable, however, that the protonolysis of F430 is predicted to be exothermic provided that the protein is slightly more polar than a continuum solvent with a dielectric constant of 4. Of course, this energy strongly depends on the proton donor.

The results in the previous sections indicate that if a Ni–Me complex should form in MCR, it should be through a heterolytic reaction, ending up in $Ni^{III}HcorMeAm$. It is then more likely that the methyl group dissociates from this complex, rather than after an electron transfer reaction (which would give the same problems as for the homolytic $Ni^{I/II}$ reaction). We have modelled such a reaction by a simple hydrolysis:

$$M^{III}RMeIm/Am + H_2O \rightarrow M^{III}ROHIm/Am + CH_4 \tag{9}$$

The resulting hydrolysis energies are presented in Table 18. It can be seen that this reaction is exothermic (by 33–93 kJ/mole) for all complexes. Hydrolysis of the Hcor complexes is less exothermic for Ni than for Co, whereas the opposite is true for the Cor complexes. The results for the two axial ligands are similar. As a result, the hydrolysis energies for the B_{12} and F430 models are almost identical, 40–60 kJ/mole. Thus, we can conclude that provided that a proper methyl donor is employed, heterolytic methyl transfer followed by hydrolysis is a possible reaction scheme for MCR, at least considering the reaction energies.

Reduction potentials

One of the most important aspects of transition-metal complexes is their reduction potentials. This is quite obvious for the present complexes, which are all assumed to be redox active in the reaction mechanism of the corresponding enzymes. Therefore, we have examined the reduction potential of several of the complexes in this investigation.

We first look at the reduction potentials of the $M^{II/III}RIm_2$ complexes in Table 19 (all reported potentials are relative to the standard hydrogen electrode). As usual for processes changing the charge of the complexes, the potentials vary strongly with the solvation, but the relative values for the various metals and ring systems are quite constant. The largest difference is between Por and the other ring systems (3 V lower potentials in vacuum, but only ~0.3 V in solution), which of course is a result of the double negative charge of Por. On the other hand, there is no clear difference between Cor and Hcor.

The trend for the metal ions is also pronounced: The reduction potential of Co is

always ~0.7 V smaller than that of Fe. On the other hand, the potential of Fe is ~0.2 V lower than that of Ni (with the exception of $NiCorIm_2$). This is in accordance with the general conclusion that the M^{III} state of Ni is less accessible than for the other two metals. Thus, even in water solution, the $NiHcorIm_2$ complex has an estimated reduction potential of 0.1 V, whereas the other two native complexes ($FePorIm_2$ and $CoCorIm_2$) both have potentials of –0.5 to –0.9 V. The calculated potentials are slightly lower than experimental potentials, which are –0.4 to +0.1 V for His_2 ligated cytochromes.[85]

A natural way to change these potentials is to modify the axial ligands. An introduction of a negatively charged ligand can be expected to decrease the potentials (stabilise the oxidised state) and this is also seen for the $M^{II/III}RMeIm/Am$ complexes (Table 20). Here, the difference between Co and Ni is only 0.1 V in Cor and ~0.3 in Hcor. The potentials are more negative in Cor than in Hcor, by 0.1 V for Co and ~0.3 V for Ni. Im gives slightly lower potentials than Am (by ~0.1 V). In total, the F430 model has a 0.5 V more positive potential than the B_{12} model.

However, it is also interesting to look at the $M^{I/II}$ complexes, which have been implicated in the reaction mechanisms of both F430 and B_{12}. The reduction potentials of the $M^{I/II}R$ complexes are listed in Table 21. They are more negative than the $M^{II/III}Im_2$ potentials, but less negative than the $M^{II/III}MeIm/Am$ potentials, indicating that the M^I state is less favoured. As for the $M^{II/III}Im_2$ complexes, the Por ring gives much more negative potentials than the other two rings, which have similar potentials. However, the trends for the metals are completely different. For the $M^{I/II}$ couple, the reduction potentials follow the trend Ni < Fe < Co, i.e. the inverse of that found for the $M^{II/III}$ couple. The differences are 0.2–0.4 V and as a result, the F430 model has a ~0.5 V more negative potential than the B_{12} model (again disregarding $Ni^{II}Cor$). Thus, the results confirm the stability of Co^I state, which is employed in the reactions of methylcobalamin. On the other hand, we see no indication of a stabilisation of the Ni^I state in these systems. On the contrary, the Ni^I predicted to be even less stable than Fe^I. This is in accordance with previous computational results[36] and also with the general inorganic picture that Ni^{II} is the dominating oxidation state of Ni.[85]

Reorganisation energies

Finally, we have looked at a typical reaction of the haem enzymes, namely electron transfer, performed by the cytochromes. According to the semi-classical

85 J. J. R. Fraústo da Silva, R. J. P. Williams, The biological chemistry of the elements, Clarendon Press, Oxfor, 1994.

Marcus theory[86], the rate of electron transfer depends on three terms, the reduction potential, the electronic coupling (which depends mainly on the distance between the donor and acceptor sites), and the reorganisation energy (λ). The latter term describes how much the geometry of the donor and acceptor sites change during electron transfer. It is normally divided into two contributions, the inner- and outer-sphere reorganisation energy (λ_i and λ_o), depending on what atoms are relaxed. For a metal-containing protein, the inner-sphere reorganisation energy is associated with the structural change of the first coordination sphere, whereas the outer-sphere reorganisation energy involves structural changes of the remaining protein as well as the solvent. Therefore, we study λ_i as a measure of the intrinsic self-exchange reorganisation energy of a given complex.

We have calculated the inner-sphere reorganisation energy of $M^{II/III}RIm_2$ for all three ring systems with Co, Ni, and Fe. It is calculated as the energy difference of the reduced complex at its optimum geometry and at the optimum geometry of the oxidised complex (λ_{red}) or vice versa (λ_{ox}).[80,87] For a self-exchange reaction, $\lambda_i = \lambda_{red} + \lambda_{ox}$. This approach has been successfully applied in a series of studies[16,80,88,89,90], in particular for the calculation of λ_i for cytochrome models with various sets of axial ligands.[21]

The reorganisation energies are shown in Table 22. It can be seen that Fe gives low reorganisation energies in all three ring systems, although it is appreciably higher in the Hcor ring (23 kJ/mole) than in the other two ring systems (3–5 kJ/mole). The reason why the reorganisation energy is so low is that the reduction involves only occupation of a $3d$ orbital that is not directed towards any ligand, as has been discussed before.[16] The relatively high reorganisation energies in Hcor ring is caused by the flexibility of this ring, which allows for a larger change in the Fe–N_{eq} distances (0.02 Å on average, cf. Table 23) than for the other rings (0.002 Å). Therefore, Hcor would be a suboptimal choice for an electron carrier.

Co gives a high reorganisation energy in all rings. As has been discussed before,[16] this is because Co^{II}, in variance to Co^{III}, has one electron in the $3d_{z^2}$ orbital, leading to very different Co–N_{Im} distances for the two oxidation states, e.g. 1.96 and 2.30–2.34 Å in the Hcor complexes (Table 23).

The reorganisation energy for Ni (23–54 kJ/mole) is higher than of Fe, but appreciably lower than for Co. This is caused by the change in the spin state of Ni^{II} (HS)

86 Marcus, R. A.; Sutin, N. *Biochim. Biophys. Acta* **1985**, *811*, 265-322.
87 Klimkans, A.; Larsson, S. *Chem. Phys. Lett.* **1994**, *189*, 25-31.
88 Ryde, U.; Olsson, M. H. M. *Intern. J. Quant. Chem.* **2001**, *81*, 335-347.
89 Sigfridsson, E.; Olsson, M. H. M.; Ryde, U. *Inorg. Chem.* **2001**, *40*, 2509-2519.
90 M. H. M. Olsson, U. Ryde, J. Am. Chem. Soc. **2001**, *123*, 7866-7876.

and Ni^{III} (LS), which leads to quite extensive changes in the $Ni–N_{eq}$ distances (e.g. from 2.10 to 2.00 Å in Hcor). Hcor, once again also gives higher reorganisation energies than the other two ring systems. Thus, we can conclude that $Fe^{II/III}Por$ is the ideal choice for an electron-transfer site (although FeCor would do as well, at a more positive potential), whereas the other metals and the Hcor ring would give higher reorganisation energies and therefore a poorer site.

Concluding remarks

In this article, we have compared various chemical properties and functional aspects of the three common tetrapyrroles in biology, haem, coenzyme B_{12}, and coenzyme F430. We have collected a great amount of data, presented in Tables 1–23 and discussed it in some detail in the previous sections. In this section, we will point out the most interesting results.

First, we have shown (Figure 5) that the size of the central cavity in the various ring systems follows the trend Cor < Por ≈ Chl < Bchl < Ibc < Hcor. This should be compared to the sizes of the various metal ions, which can be estimated from the average $M–N_{eq}$ bond lengths in the ring-cut PMod complexes in Table 8: IS Fe^{II} < LS Co^{II} < LS Ni^{II} ≈ LS Co^{I} < LS Fe^{I} << LS Ni^{I} for the four-coordinate complexes and LS Fe^{III} ≈ LS Co^{II} < LS Co^{III} < LS Ni^{III} < LS Fe^{II} << LS Ni^{II} for the six-coordinate Im_2 complexes. Consequently, Cor fit the ionic radii of all three oxidation states of LS Co nicely whereas the cavity of the Por ring is too large for LS Fe and therefore stabilises the IS and HS states, as has already been pointed out.[16] Moreover, the results indicate that Hcor has been selected to allow for the large sizes of the Ni ion, especially in its HS Ni^{II} state.

Consequently, we can conclude that the ring systems have probably been mainly selected to fit their respective metal ions, which is also supported by the fact that nearly all native combinations of metals and ring systems are more stable than other combinations (Tables 3 and 4).

Figure 5 also shows that the flexibility of the rings follows the trend Hcor > Cor > Por ≈ Ibc > Chl > Bchl. In particular, the results show that the Hcor ring allows for large distortions by major changes in the conformation of the ring. This is illustrated by very long distances in some LS Ni^{II} complexes with e.g. 2.78 Å for LS $Ni^{II}HcorMeIm$.

We have also studied the binding of neutral axial ligands to the various metals and showed that the Gln residue, present in the MCR enzyme, probably provides and ideal weak ligand to the metal site, thereby stabilising the $Ni^{II/III}$ states. However, it binds very

weakly to the Ni^I state and has quite restricted influence on the studied reaction energies.

Finally, we have looked at some functional aspects of the cofactors. First, we have tested if it is possible that coenzyme F430 forms a Ni–Me bond during the MCR reaction cycle, as has been assumed in most suggested reaction mechanisms[78], but has been challenged in a recent theoretical study.[37] Our results show that it is highly unlikely that a $Ni^{II/III}$–Me complex is formed by a homolytic reaction, in accordance with previous theoretical results.[37] Moreover, the heterolytic methyl transfer, which actually takes place for several MeCbl enzymes, is ~70 kJ/mole less favourable for coenzyme F430 than for B_{12}. However, with a proper choice of the methyl donor, e.g. a protonated coenzyme M, a proton transfer reaction would still be exothermic. Thus, our results indicate that it is too early to rule out a Ni^{III} – Me intermediate in the reaction mechanism of MCR.

In fact, the results in this article show that coenzyme F430 seems to be designed to stabilise the Ni^{II} and Ni^{III} states of the coenzyme, indicating that the binding of Me is actually desirable. Moreover, our results show that once a Ni^{III}HcorMeAm complex is formed, it is readily hydrolysed to form methane and a Ni^{III}HcorOHAm complex. The latter complex can finally oxidise coenzyme M and B to a heterodisulphide: The reaction in Eqn. 10

$$Ni^{III}HcorOHAm^+ + MeSH + MeS^- \rightarrow Ni^IHcor + H_2O + Am + MeSSMe \qquad (10)$$

is predicted to be exothermic by 389–767 kJ/mole (water solution and vacuum). Thus, we see that a reaction mechanism involving a heterolytic methyl transfer from a protonated coenzyme M to Ni^I–F430 is exothermic throughout. The only problem is to ensure that coenzyme M is protonated (and that the proton on coenzyme B is properly taken away in Eqn. 10, but this is probably a smaller problem, because this reaction is so exothermic). In this respect, the structure of methyl coenzyme M is interesting: Its full structure is $Me–S–CH_2–CH_2–SO_3^-$. Thus, there is a negatively charged group less than 5 Å from the sulphur atom to be protonated. Such an unusual molecule could have been selected to facilitate its protonation, thereby making the methyl transfer energetically allowed. However, at present all these suggestions are mere speculations that need to be confirmed by a detailed study of the reaction mechanisms in the protein. It should also be mentioned that Pelmenshikov et al. have suggested a plausible and energetically possible reaction mechanism (including activation energies) without any

Ni–Me intermediate.[37]

Second, we have looked at the electron-transfer properties of the cofactors. In general, the reduction potential of the $M^{I/II0}$ couple follows the Ni < Fe < Co, whereas the $M^{II/III}$ couple follows the opposite trend, Co < Fe < Ni. In both cases, this confirms the experimental observation that the +II state is most stable for Ni, whereas the I state is stabilised for Co and the III state is more stable for Fe. However, it was quite unexpected that the Ni^I state, which is observed in MCR, actually is less stable than the Fe^I state, with any ring system.

Finally, we have looked at the reorganisation energies and shown that the $Ni^{II/III}$ couple in its ground state is not very well fitted for electron transfer, owing to quite extensive changes in the bond lengths between the metal and the N_{eq} atoms. Likewise, the Hcor is too flexible for an ideal electron carrier. Thus, our calculations rationalise the observation that the $Fe^{II/III}Por$ is still the best combination for electron transfer.

A conspicuous observation in this paper is that Ni is appreciably more complicated to treat with theoretical methods than the other two metal ions, at least for complexes of the type studied in this paper. The reason for this is the presence of competing spin states (LS and HS) of similar energy for both Ni^{III} and, especially, Ni^{II}, but also the flexibility of the spin states in all the oxidation states of Ni. Thus, we have in several cases, e.g. for the OH^- or Me^- complexes (cf. Table 10), but also for Ni^ICor, found alternative electronic configurations, even within series of analogous complexes and we have confirmed that these often differ by less than 10 kJ/mole.

Even worse, we have also shown that different density functional methods give very different (~50 kJ/mole) relative energies of the various spin states. This is of course a serious problem in an investigation like this, especially as we predict (in accordance with experiments on MCR) that the spin state of the Ni ion changes with the oxidation state of the metal (LS for four-coordinate Ni^I and Ni^{II} complexes, HS for five- and six-coordinate Ni^{II}, but LS again for Ni^{III}). It is conceivable that some of the results, especially for the BDEs, hydrolysis, and protonolysis energies, are quite uncertain and may change considerably if other theoretical methods were used. However, we still believe that the present results provide significant advancement in our understanding of the differences and similarities of the tetrapyrrole cofactors in nature.

Table 1. Comparison of the Ni – N_{eq} distances, Mulliken charge on Ni (Q), and spin density on Ni (SD) of the four-coordinate Ni complexes with Hcor, HcorMe$_2$, and its C12, C13 diepimer. Hcor – planar is an alternative structure of Ni^{I}Hcor with a nearly planar Hcor ring (like that of Ni^{I}HcorMe$_2$) and a 0.4 kJ/mole higher energy (cf. Figure 3).

Metal	Ring	Ni–N1	Ni–N2	Ni–N3	Ni–N4	Q	SD
Ni^I	Hcor	2.059	2.094	1.998	2.008	0.223	0.863
	Hcor – planar	2.061	2.137	1.996	2.000	0.219	0.830
	HcorMe$_2$ (planar)	2.051	2.139	1.998	1.999	0.211	0.816
	HcorMe$_2$ diepimer	2.049	2.101	2.000	2.011	0.215	0.857
Ni^{II}	Hcor	1.922	1.969	1.896	1.935	0.415	–
	HcorMe$_2$	1.927	1.966	1.886	1.929	0.414	–
	HcorMe$_2$ diepimer	1.917	1.967	1.893	1.933	0.405	–

Table 2. Spin-splitting energies of all the studied complexes. Values in brackets for LS states are for open-shell singlets, whereas those for the NiRIm$_2$ complexes are B3LYP energies. Values in bold face indicates that the Im or Am ligand has dissociated.

Complex	Ring	Fe			Co		Ni	
		LS	IS	HS	LS	HS	LS	HS
M^{I}R	Por	0.0	–	51.8	0.0	69.1	0.0	–
	Cor	0.0	–	68.4	0.0	95.4	0.0	–
	Hcor	0.0	–	57.8	0.0	77.7	0.0	–
M^{I}RIm	Cor		–		**0.0**	68.9	**0.0**	–
	Hcor		–		**0.0**	51.3	**0.0**	–
M^{I}RAm	Cor		–		**0.0**	95.1	**0.0**	–
	Hcor		–		**0.0**	58.6	**0.0**	–
M^{II}R	Por	47.2	0.0	70.8	0.0	83.2	0.0	99.9
	Cor	44.0	0.0	154.5	0.0	151.0	0.0	157.3
	Hcor	45.8	0.0	69.4	0.0	82.3	0.0	102.7
M^{II}RIm	Cor				0.0		**-89.4**	0.0
	Hcor				0.0	59.0	**-19.8**	0.0
M^{II}RAm	Cor				0.0	133.1	**-103.1 (-105.8)**	0.0
	Hcor				0.0	107.8	**-48.9**	0.0
M^{II}RMe	Por	0.0	65.0	137.4	0.0	99.2	51.3	0.0
	Cor	0.0	81.2	167.4	0.0	115.0	16.0	0.0
	Hcor	0.0	68.4	90.2	0.0	52.9	64.6	0.0
M^{II}ROH	Por	0.0			0.0	6.3	85.6 (37.5)	0.0
	Cor	0.0			0.0	53.4	33.6 (13.4)	0.0
	Hcor	0.0			0.0	21.7	25.4 (33.3)	0.0
M^{II}RIm$_2$	Por	0.0			0.0		**-17.9 (25.8)**	0.0
	Cor	0.0			0.0		**-72.6 (-26.2)**	0.0
	Hcor	0.0			0.0		**-35.1 (24.6)**	0.0
M^{II}RImMe	Cor				0.0	**119.2**	17.9 (12.8)	0.0
	Hcor				0.0	**62.6**	-2.8 (-3.5)	0.0[a]
M^{II}RAmMe	Cor				0.0	**113.4**	12.4 (7.7)	0.0[b]
	Hcor				0.0		**-0.8 (-0.8)**	0.0[b]
M^{III}RImMe	Cor	0.0	115.2	260.5	0.0	165.7	0.0	182.1
	Hcor				0.0		0.0	156.7
M^{III}RAmMe	Cor				0.0	162.3	0.0	176.5
	Hcor				0.0	103.6	0.0	133.8
M^{III}RImOH	Cor				0.0		0.0	80.2

Complex	Ring	Fe	Co		Ni	
	Hcor		0.0	90.6	0.0	55.2
$M^{III}RAmOH$	Cor		0.0		0.0	80.1
	Hcor		0.0	60.2	0.0	46.6
$M^{III}RIm_2$	Por	0.0	0.0		0.0	39.1 (-15.9)
	Cor	0.0	0.0		0.0	106.5 (53.2)
	Hcor	0.0	0.0		0.0	31.2 (-25.2)

[a] In this complex, the $Co–N_{Im}$ bond was constrained to 2.16 Å (the optimum distance of the $Ni^{II}CorImMe$ complex, which did not dissociate. Dissociated complexes are 29 kJ/mole more stable.

[b] In these two complexes, the $Co–O_{Am}$ bond was constrained to 2.26 Å (the optimum distance of the $Ni^{II}CorAmMe$ complex, which did not dissociate. Dissociated complexes are 29 and 24 kJ/mole more stable.

Table 3. Thermodynamic stabilities of various combinations of monovalent metals and rings, calculated from Eqn. 2. The native combinations are marked in bold face.

# Reaction	$M^I R$			$M^{II}R$	$M^{II}RMe$	$M^{II}RIm_2$	$M^{III}RIm_2$
	$\varepsilon = 1$	$\varepsilon = 4$	$\varepsilon = 80$	$\varepsilon = 1$	$\varepsilon = 1$	$\varepsilon = 1$	$\varepsilon = 1$
1 **FePor** + **CoCor** → FeCor + CoPor	**23.6**	**15.5**	**12.7**	**17.7**	**-7.0**	**5.3**	**11.2**
2 **FePor** + CoHcor → FeHcor + CoPor	17.0	13.0	7.9	5.5	-2.8	11.4	-11.3
3 FeHcor + **CoCor** → FeCor + CoHcor	6.6	2.6	4.8	12.3	-4.2	-6.1	22.6
4 **FePor** + NiCor → FeCor + NiPor	0.1	-15.0	-19.2	32.6	-40.9	-51.2	22.2
5 **FePor** + **NiHcor** → FeHcor + NiPor	**32.2**	**29.9**	**26.1**	**16.5**	**43.3**	**19.4**	**9.9**
6 FeCor + **NiHcor** → FeHcor + NiCor	32.1	44.9	45.3	-16.1	84.1	70.7	-12.3
7 NiPor + **CoCor** → NiCor + CoPor	23.5	30.5	31.9	-14.9	33.9	56.6	-11.0
8 **NiHcor** + CoPor → NiPor + CoHcor	15.3	16.9	18.2	11.0	46.0	8.0	21.2
9 **NiHcor** + **CoCor** → NiCor + CoHcor	**38.7**	**47.4**	**50.1**	**-3.8**	**79.9**	**64.6**	**10.3**

Table 4. Thermodynamic stability of Co/Ni Cor/Hcor complexes with various axial ligands, calculated from Eqn. 3.

Oxidation state	Axial Ligands		Reaction energy (kJ/mole)		
	X	Y	$\varepsilon = 1$	$\varepsilon = 4$	$\varepsilon = 80$
I	–	–	38.7	47.4	50.1
I	Im	–	52.1	57.5	61.8
I	Am	–	53.0	53.6	54.0
II	–	–	-3.8	-4.5	-5.4
II	Me	–	79.9	75.7	72.6
II	OH	–	51.3	51.7	51.7
II	Im	–	70.9	71.5	72.1
II	Am	–	53.4	51.3	50.0
II	Im	Me	70.6	74.6	77.8
II	Am	Me	84.4	89.9	93.4
II	Im	Im	64.6	66.8	68.4
III	Im	Me	54.6	54.7	54.6
III	Am	Me	64.6	68.0	69.1
III	Im	OH	29.4	25.7	23.2
III	Am	OH	24.2	15.6	9.9
III	Im	Im	10.3	7.7	6.3

Table 5. Spin densities for the various complexes without or with weak axial ligands.

Metal	Ring	Axial Ligand	Spin density Metal	Ring	Axial ligand
Fe^{I}	Por	–	1.76	-0.76	
	Cor	–	1.52	-0.52	
	Hcor	–	1.40	-0.40	
Ni^{I}	Por	–	0.98	0.02	
	Cor	–	0.21	0.79	
	Hcor	–	0.86	0.14	
Fe^{II}	Por	–	2.16	-0.16	
	Cor	–	2.07	-0.07	
	Hcor	–	2.09	-0.09	
Co^{II}	Por	–	1.14	-0.14	
		Im_2	0.98	-0.11	0.07, 0.07
	Cor	–	1.13	-0.13	
		Am	1.03	-0.09	0.06
		Im	0.95	-0.06	0.10
		Im_2	0.96	-0.11	0.08, 0.07
	Hcor	–	1.09	-0.09	
		Am	1.03	0.06	-0.08
		Im	0.96	-0.06	0.09
		Im_2	0.95	-0.08	0.07, 0.06
Ni^{II}	Por	Im_2	1.48	0.35	0.08, 0.08
	Cor	Am	1.44	0.46	0.10
		Im	1.41	0.47	0.12
		Im_2	1.43	0.38	0.09, 0.09
	Hcor	Am	1.49	0.41	0.10
		Im	1.46	0.42	0.12
		Im_2	1.47	0.36	0.09, 0.08
Fe^{III}	Por	Im_2	0.97	0.02	0.00, 0.00
	Cor	Im_2	0.85	0.19	-0.02, -0.02
	Hcor	Im_2	0.77	0.26	-0.01, -0.01
Ni^{III}	Por	Im_2	0.70	0.02	0.14, 0.14
	Cor	Im_2	0.67	0.03	0.15, 0.15
	Hcor	Im_2	0.74	0.00	0.13, 0.13

Table 6. Energies of the HOMO and LUMO orbitals, as well as the energies gap (in eV) of the four-coordinate $M^I R$ complexes in their ground states.

Ring	Metal	E_{HOMO}	E_{LUMO}	$E_{LUMO}-E_{HOMO}$
Por	Fe	0.23	1.03	0.80
	Co	0.16	1.05	0.89
	Ni	0.70	0.91	0.21
Cor	Fe	-2.90	-2.02	0.87
	Co	-3.04	-1.83	1.21
	Ni	-2.34	-1.92	0.41
Hcor	Fe	-3.17	-2.24	0.93
	Co	-3.26	-1.98	1.27
	Ni	-2.90	-2.06	0.84

Table 7. Metal–ligand distances, out-of-plane distances, and corrin fold angles for the four-coordinate M^I complexes.

Ring	M	M–N_{eq1}	M–N_{eq2}	M–N_{eq3}	M–N_{eq4}	Fold angle	Out-of-plane distance
Por	Fe^I	1.987	1.987	1.987	1.987	–	0.000
	Co^I	1.968	1.968	1.968	1.968	–	0.000
	Ni^I	2.031	2.031	2.031	2.031	–	0.000
Cor	Fe^I	1.929	1.861	1.929	1.861	4.9	0.074
	Co^I	1.901	1.835	1.901	1.835	6.0	0.099
	Ni^I	1.923	1.867	1.928	1.888	13.3	0.096
Hcor	Fe^I	1.977	1.974	1.931	1.961	–	0.246
	Co^I	1.937	1.935	1.889	1.924	–	0.269
	Ni^I	2.059	2.094	1.998	2.008	–	0.184

Table 8. The average $M–N_{eq}$ distances in the $M^{I/II}R$ and $M^{II/III}RIm_2$ complexes, compared to those involving the strain-free PMod, CMod, and HMod broken-ring models.

Ligands	Metal	Average $M–N_{eq}$ distances (Å)					
		PMod	Por	CMod	Cor	HMod	Hcor
–	Fe^I	1.878	1.987	1.886	1.895	1.889	1.961
	Co^I	1.872	1.968	1.853	1.868	1.858	1.921
	Ni^I	1.994	2.031	1.924	1.901	1.947	2.040
–	Fe^{II}	1.844	1.992	1.916	1.907	1.912	1.973
	Co^{II}	1.857	1.982	1.885	1.898	1.881	1.952
	Ni^{II}	1.869	1.971	1.874	1.884	1.873	1.930
Im_2	Fe^{II}	1.941	2.007	1.931	1.919	1.935	2.004
	Co^{II}	1.918	2.003	1.919	1.909	1.917	1.992
	Ni^{II}	2.068	2.064	2.093	1.978	2.092	2.102
Im_2	Fe^{III}	1.913	2.009	1.945	1.921	1.938	1.982
	Co^{III}	1.926	2.005	1.937	1.924	1.939	1.989
	Ni^{III}	1.920	2.010	1.970	1.925	1.960	2.003

Table 9. Average M–N$_{eq}$ distances in the various complexes. Complexes, marked in bold face have a differing electronic state.

Axial Ligands	Metal	Average M–N$_{eq}$ distances (Å)		
		Por	Cor	Hcor
Me	Fe^{II}	1.984	1.891	1.972
	Co^{II}	1.992	1.901	**1.983**
	Ni^{II}	**2.063**	**1.947**	**2.084**
OH	Fe^{II}	1.993	1.899	1.973
	Co^{II}	**1.998**	**1.897**	**1.961**
	Ni^{II}	**2.065**	**1.959**	**2.080**
Im	Co^{II}		1.907	1.993
	Ni^{II}		1.982	2.091
Am	Co^{II}		1.904	1.980
	Ni^{II}		1.977	2.082
MeIm	Co^{II}		1.919	2.102
	Ni^{II}		1.980	**2.099**
MeAm	Co^{II}		1.911	2.061
	Ni^{II}		1.972	**2.094**
MeIm	Co^{III}		1.908	1.987
	Ni^{III}		1.970	2.087
MeAm	Co^{III}		1.902	2.010
	Ni^{III}		1.959	2.087
OHIm	Co^{III}		1.917	1.976
	Ni^{III}		**1.914**	2.065
OHAm	Co^{III}		1.913	1.970
	Ni^{III}		**1.908**	**1.956**

Table 10. M–Me and M–OH bond lengths in the various complexes. As is discussed in the text, there is one group of complexes with short M–Me/OH distances and another with longer distances. The longer distance are marked in bold face in this table.

Ring	Metal	Me					OH		
		$M^{II}R$	$M^{II}RIm$	$M^{II}RAm$	$M^{III}RIm$	$M^{III}RAm$	$M^{II}R$	$M^{III}RIm$	$M^{III}RAm$
Por	Fe	1.975					1.853		
	Co	1.943					**1.991**		
	Ni	**2.065**					**1.956**		
Cor	Fe	1.986					1.872		
	Co	1.952	1.968	1.960	1.980	1.971	**2.032**	1.883	1.867
	Ni	**2.102**	1.961	1.991	1.973	1.977	**1.981**	**2.023**	**2.017**
Hcor	Fe	1.985					1.897		
	Co	**2.047**	1.975	1.956	1.979	1.963	**2.049**	1.890	1.873
	Ni	**2.057**	**2.062**	**2.071**	1.965	1.957	**1.978**	1.881	**2.014**

Table 11. Spin densities for the various complexes with strong axial ligands. Complexes with long M–OH/Me distances are marked in bold face.

Metal	Ring	Ligand OH/Me	Ligand Im/Am	Spin density on			
				Metal	Ring	OH/Me	Im/Am
Co^{II}	Por	Me	–	0.03	0.97	-0.01	
	Cor	Me	–	0.05	0.96	-0.01	
			Am	0.00	0.95	0.06	0.00
			Im	0.05	0.95	-0.01	0.00
	Hcor	Me	–	**0.70**	**0.14**	**0.16**	
			Am	0.71	0.37	-0.08	0.00
			Im	0.95	0.12	-0.07	-0.01
Ni^{II}	Por	Me	–	**1.23**	**0.45**	**0.32**	
	Cor	Me	–	**0.86**	**0.74**	**0.40**	
			Am	0.82	1.14	0.03	0.01
			Im	0.73	1.33	-0.07	0.01
	Hcor	Me	–	**1.29**	**0.37**	**0.34**	
			Am	**1.29**	**0.43**	**0.27**	**0.02**
			Im	**1.24**	**0.54**	**0.19**	**0.04**
Ni^{III}	Cor	Me	Am	0.70	0.32	-0.03	0.01
			Im	0.71	0.35	-0.07	0.01
	Hcor	Me	Am	0.79	0.30	-0.09	0.00
			Im	0.77	0.31	-0.09	0.00
Co^{II}	Por	OH	–	**0.96**	**-0.18**	**0.22**	
	Cor	OH	–	**0.86**	**-0.09**	**0.23**	
	Hcor	OH	–	**0.88**	**-0.06**	**0.18**	
Ni^{II}	Por	OH	–	**1.48**	**0.23**	**0.30**	
	Cor	OH	–	**1.26**	**0.48**	**0.31**	
	Hcor	OH	–	**1.46**	**0.33**	**0.22**	
Ni^{III}	Cor	OH	Am	**0.51**	**0.05**	**0.41**	**0.03**
			Im	**0.53**	**0.04**	**0.39**	**0.05**
	Hcor	OH	Am	**0.61**	**0.05**	**0.33**	**0.01**
			Im	0.70	0.29	0.01	0.01

Table 12. M–N$_{Im}$ and M–O$_{Am}$ bond lengths in the various complexes. Distances in complexes with a long M–Me/OH bond are marked in bold face.

Ring	Metal	Im				Am			
		M^{II}R	M^{II}RMe	M^{III}RMe	M^{III}ROH	M^{II}R	M^{III}RMe	M^{III}RMe	M^{III}ROH
Cor	Co	2.155	2.173	2.190	2.032	2.209	2.368	2.289	2.096
	Ni	2.050	2.143	2.141	**2.490**	2.078	2.258[a]	2.282	**2.591**
Hcor	Co	2.145	2.114	2.148	2.010	2.225	2.248	2.250	2.071
	Ni	2.057	**2.157[b]**	2.110	2.019	2.096	**2.258[a]**	2.166	**2.988**

[a] This distance was fixed in these calculations.

Table 13. The affinity of the axial ligands Im or Am to the four-coordinate $M^{I/II}$ complexes.

Ligand	Ring	Metal	$M^{II}R$			$M^{II}RMe$	$M^{II}RIm$
			$\varepsilon = 1$	$\varepsilon = 4$	$\varepsilon = 80$	$\varepsilon = 1$	$\varepsilon = 1$
Im	Cor	Co	-85.1	-63.9	-52.2	-26.7	-33.9
		Ni	57.7	79.3	91.7	2.2	-48.0
	Hcor	Co	-74.0	-53.0	-40.2	-21.9	-58.1
		Ni	-6.0	14.3	26.1	16.3	-66.0
Am	Cor	Co	-71.6	-48.1	-35.1	-24.3	–
		Ni	66.0	88.3	100.6	0.5	–
	Hcor	Co	-68.9	-48.1	-35.8	-8.0	–
		Ni	11.4	32.5	44.4	12.3	–

Table 14. Homolytic M^{II}–C bond dissociation energies for the five-coordinate $M^{II}RMe$ complexes, as defined in Eqn. 4.

Ring	Metal	M–C BDE (kJ/mole)		
		$\varepsilon = 1$	$\varepsilon = 4$	$\varepsilon = 80$
Por	Fe	162.6	157.6	154.1
	Co	97.9	82.0	68.6
	Ni	65.9	58.0	52.0
Cor	Fe	171.0	167.3	164.9
	Co	75.7	69.7	61.0
	Ni	33.2	41.1	38.8
Hcor	Fe	166.9	162.1	159.4
	Co	82.5	76.3	72.9
	Ni	81.2	76.0	73.1

Table 15. Homolytic M^{III}–C bond dissociation energies for the six-coordinate $M^{III}RLMe$ complexes, as defined in Eqn. 5.

Compound			M–C BDE (kJ/mole)		
Metal	Ring	Axial L	$\varepsilon = 1$	$\varepsilon = 4$	$\varepsilon = 80$
Co^{III}	Cor	Im	155.7	153.4	152.2
		Am	160.4	157.2	155.6
	Hcor	Im	165.9	166.1	167.4
		Am	149.2	141.6	138.5
Ni^{III}	Cor	Im	128.8	124.8	122.6
		Am	126.7	120.6	117.1
	Hcor	Im	122.7	120.6	120.4
		Am	126.7	121.7	119.0

Table 16. Reaction energy of the heterolytic methyl transfer between MeSMe and M^IR, as is defined in Eqn 7.

Compound			Reaction energy (kJ/mole)		
Metal	Ring	Axial Ligand	$\varepsilon = 1$	$\varepsilon = 4$	$\varepsilon = 80$
Co^{III}	Cor	Im	-429.9	-174.0	-60.1
		Am	-438.7	-186.0	-73.8
	Hcor	Im	-439.4	-176.1	-51.2
		Am	-461.2	-205.4	-84.6
Ni^{III}	Cor	Im	-508.2	-244.4	-128.2
		Am	-518.6	-257.5	-142.6
	Hcor	Im	-501.8	-239.3	-114.8
		Am	-515.3	-256.4	-134.4

Table 17. Protonolysis energies of $M^{II}RMe(L)$ complexes with or without an axial ligand, as defined in Eqn. 8.

Ring	Metal	Axial Ligand	Protonolysis energy (kJ/mole)		
			$\varepsilon = 1$	$\varepsilon = 4$	$\varepsilon = 80$
Por	Fe	–	67.5	-17.9	-57.2
	Co	–	18.4	-68.5	-109.0
	Ni	–	-66.7	-149.8	-186.8
Cor	Fe	–	398.4	118.2	-14.7
	Co	–	324.5	43.3	-90.2
		Am	277.1	2.4	-128.4
		Im	266.1	-6.4	-135.7
	Ni	–	190.6	-86.8	-217.8
		Am	256.1	-22.2	-155.2
		Im	246.1	-28.0	-158.3
Hcor	Fe	–	397.2	107.6	-32.7
	Co	–	339.8	53.7	-83.9
		Am	278.9	-4.0	-139.7
		Im	287.8	10.1	-121.8
	Ni	–	289.8	3.9	-133.6
		Am	288.9	10.0	-123.2
		Im	267.5	-8.4	-138.8

Table 18. Hydrolysis energies of $M^{III}RLMe$ complexes with an axial ligand, as defined in Eqn. 9.

L	Ring	Metal	Hydrolysis energy (kJ/mole)		
			$\varepsilon = 1$	$\varepsilon = 4$	$\varepsilon = 80$
Im	Cor	Co	-56.5	-52.9	-52.1
		Ni	-48.5	-47.8	-48.8
	Hcor	Co	-93.3	-83.6	-79.2
		Ni	-60.1	-49.5	-44.5
Am	Cor	Co	-40.2	-35.3	-33.3
		Ni	-58.8	-59.3	-61.0
	Hcor	Co	-77.9	-74.4	-73.2
		Ni	-56.1	-46.1	-41.2

Table 19. Reduction potentials for the $Me^{II/III}RIm_2$ complexes.

Ring	Metal	Reduction potential (eV)		
		$\varepsilon = 1$	$\varepsilon = 4$	$\varepsilon = 80$
Por	Fe	0.60	-0.17	-0.51
	Co	-0.15	-0.92	-1.26
	Ni	0.80	-0.04	-0.36
Cor	Fe	3.82	1.17	-0.09
	Co	3.02	0.32	-0.93
	Ni	3.27	0.63	-0.61
Hcor	Fe	3.63	1.05	-0.18
	Co	3.12	0.45	-0.84
	Ni	3.94	1.36	0.13

Table 20. Reduction potentials for the Me$^{\text{II/III}}$RLMe complexes.

Ring	Metal	Axial Ligand	Reduction potential (eV)		
			$\varepsilon = 1$	$\varepsilon = 4$	$\varepsilon = 80$
Cor	Co	Im	-0.81	-1.65	-2.02
		Am	-0.75	-1.60	-1.98
	Ni	Im	-0.74	-1.57	-1.95
		Am	-0.61	-1.47	-1.86
Hcor	Co	Im	-0.69	-1.61	-2.04
		Am	-0.61	-1.50	-1.92
	Ni	Im	-0.46	-1.33	-1.73
		Am	-0.27	-1.15	-1.55

Table 21. Reduction potentials for the Me$^{I/II}$R complexes.

Ring	Metal	Reduction potential (eV)		
		$\varepsilon = 1$	$\varepsilon = 4$	$\varepsilon = 80$
Por	Fe	-2.94	-1.81	-1.23
	Co	-2.78	-1.55	-0.88
	Ni	-3.33	-2.14	-1.51
Cor	Fe	0.40	-0.50	-0.90
	Co	0.62	-0.26	-0.61
	Ni	-0.32	-1.32	-1.70
Hcor	Fe	0.43	-0.56	-1.03
	Co	0.71	-0.22	-0.66
	Ni	0.21	-0.74	-1.18

Table 22. Reorganisation energies of the $M^{II/III}RIm_2$ complexes.

Metal	Ring	Reorganisation energies (kJ/mole)		
		λ_{ox}	λ_{red}	λ
Fe	Por	1.5	1.7	3.2
	Cor	2.7	2.0	4.7
	Hcor	12.1	11.0	23.0
Co	Por	75.8	44.9	120.7
	Cor	81.8	57.7	139.5
	Hcor	82.9	62.2	145.1
Ni	Por	5.8	16.9	22.7
	Cor	19.5	25.1	39.3
	Hcor	21.4	42.3	53.6

Table 23. Optimised geometries for the MRIm$_2$ complexes.

Metal	Ring	M–N$_{ax1}$	M–N$_{ax2}$	M–N$_{eq1}$	M–N$_{eq2}$	M–N$_{eq3}$	M–N$_{eq4}$
Fe^{II}	Por	1.988	1.988	2.007	2.007	2.007	2.007
	Cor	2.010	2.010	1.884	1.953	1.953	1.884
	Hcor	1.996	2.003	2.005	2.020	1.974	2.016
Co^{II}	Por	2.279	2.285	2.002	2.003	2.003	2.003
	Cor	2.344	2.342	1.879	1.939	1.940	1.879
	Hcor	2.300	2.337	1.995	2.022	1.952	1.996
Ni^{II}	Por	2.170	2.170	2.064	2.064	2.065	2.065
HS	Cor	2.226	2.227	1.964	1.991	1.993	1.963
	Hcor	2.157	2.203	2.092	2.155	2.061	2.101
Fe^{III}	Por	1.992	1.992	2.009	2.009	2.009	2.009
	Cor	2.021	2.021	1.879	1.960	1.962	1.881
	Hcor	2.003	2.005	1.945	2.023	1.957	2.002
Co^{III}	Por	1.954	1.955	2.005	2.005	2.005	2.005
	Cor	1.977	1.978	1.895	1.952	1.952	1.895
	Hcor	1.963	1.965	1.968	2.020	1.963	2.006
Ni^{III}	Por	2.169	2.169	2.011	2.009	2.011	2.009
LS	Cor	2.225	2.224	1.899	1.951	1.950	1.899
	Hcor	2.179	2.179	2.001	2.051	1.963	1.996
Ni^{III}	Por	2.167	2.167	2.062	2.065	2.066	2.063
HS	Cor	2.210	2.208	1.953	2.005	2.014	1.960
	Hcor	2.151	2.187	2.083	2.124	2.058	2.107

Figure 1. The three tetrapyrrole cofactors studied, a) haem *b*, b) F430, and c) cobalamin.

a)

b)

c)

R=

–CH₃   –CN

57
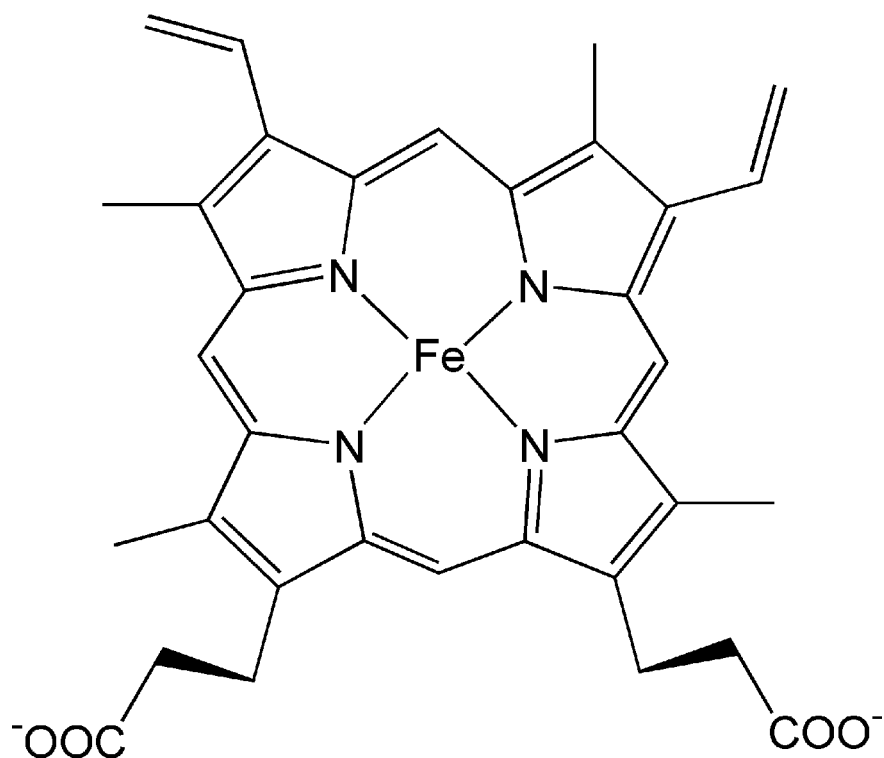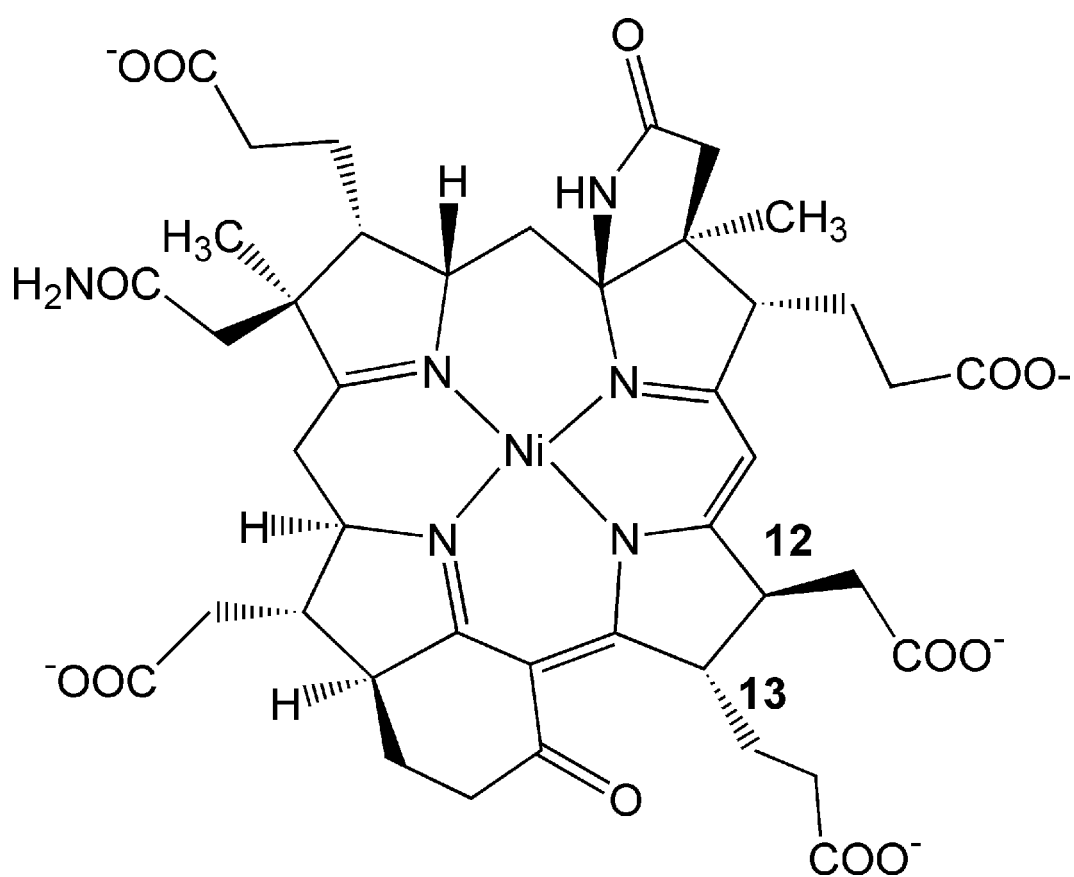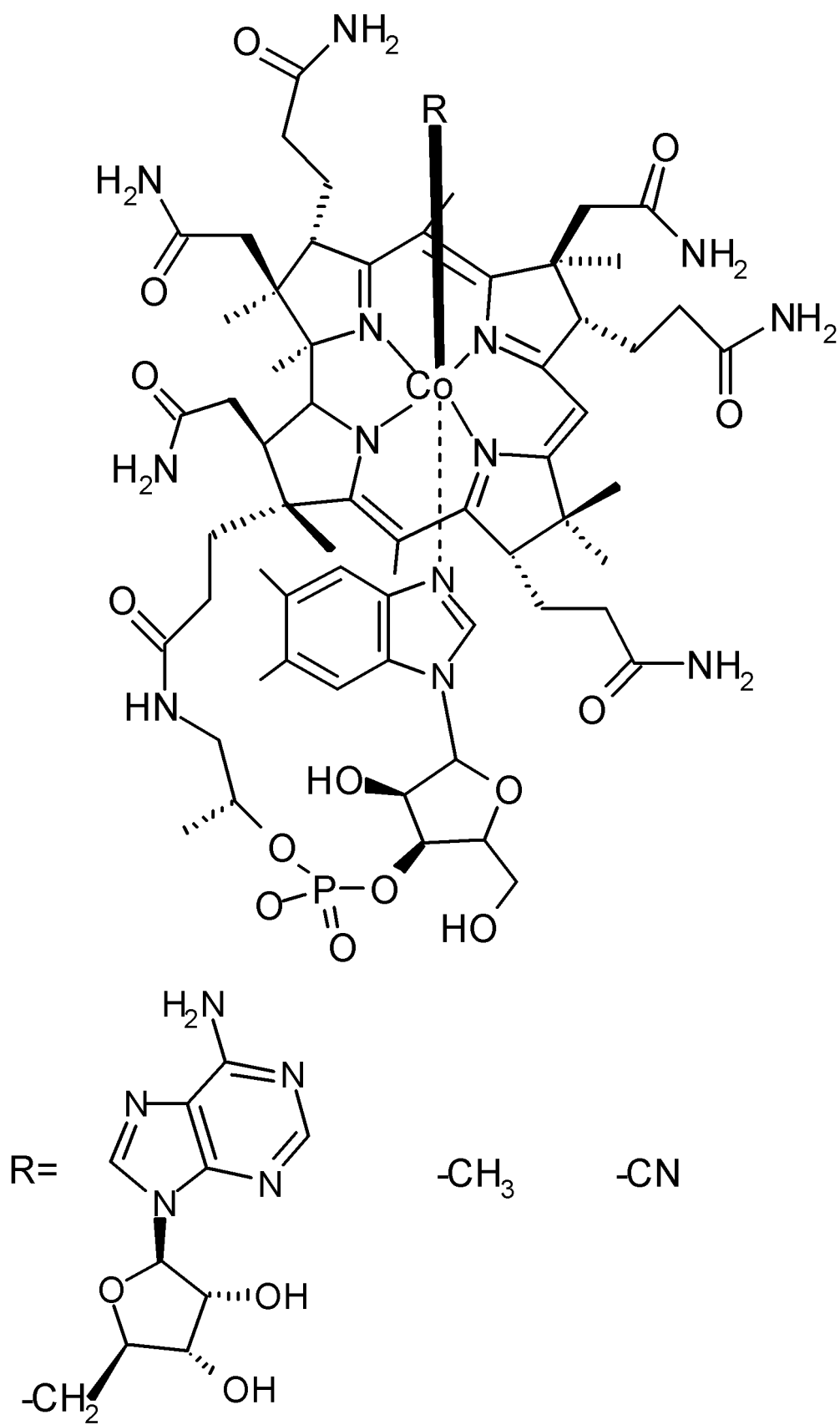
Figure 2. The optimised structures of a) Fe^{I}Por, b) Co^{I}Cor, and c) Ni^{I}Hcor.
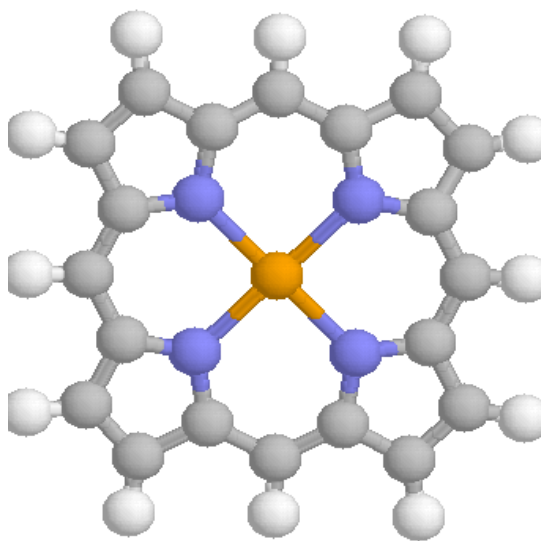
a)
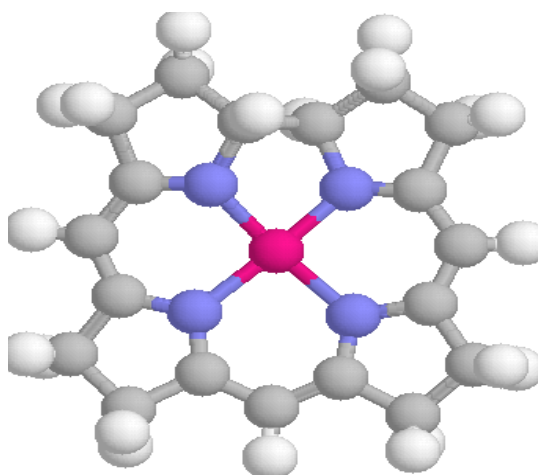
b)
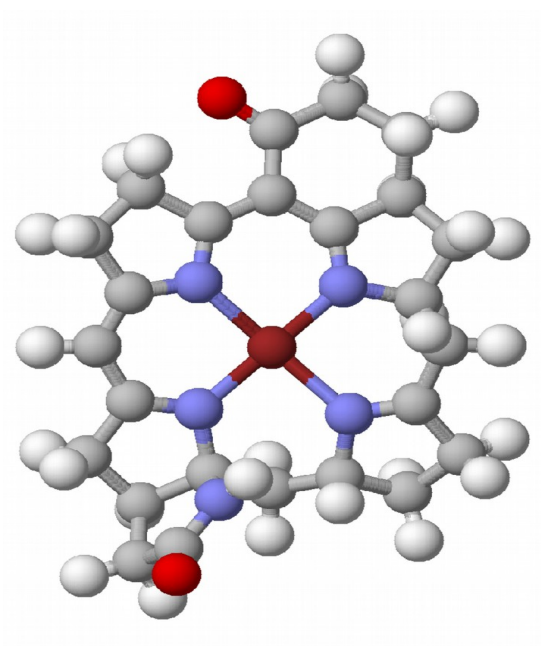
c)

Figure 3. The structure of the a) distorted (most stable) and b) planar Ni^IHcor complexes, as well as the c) normal (also planar) and d) 12,13-diepimeric $Ni^IHcorMe_2$ complexes.

a)

b)

c)

d)
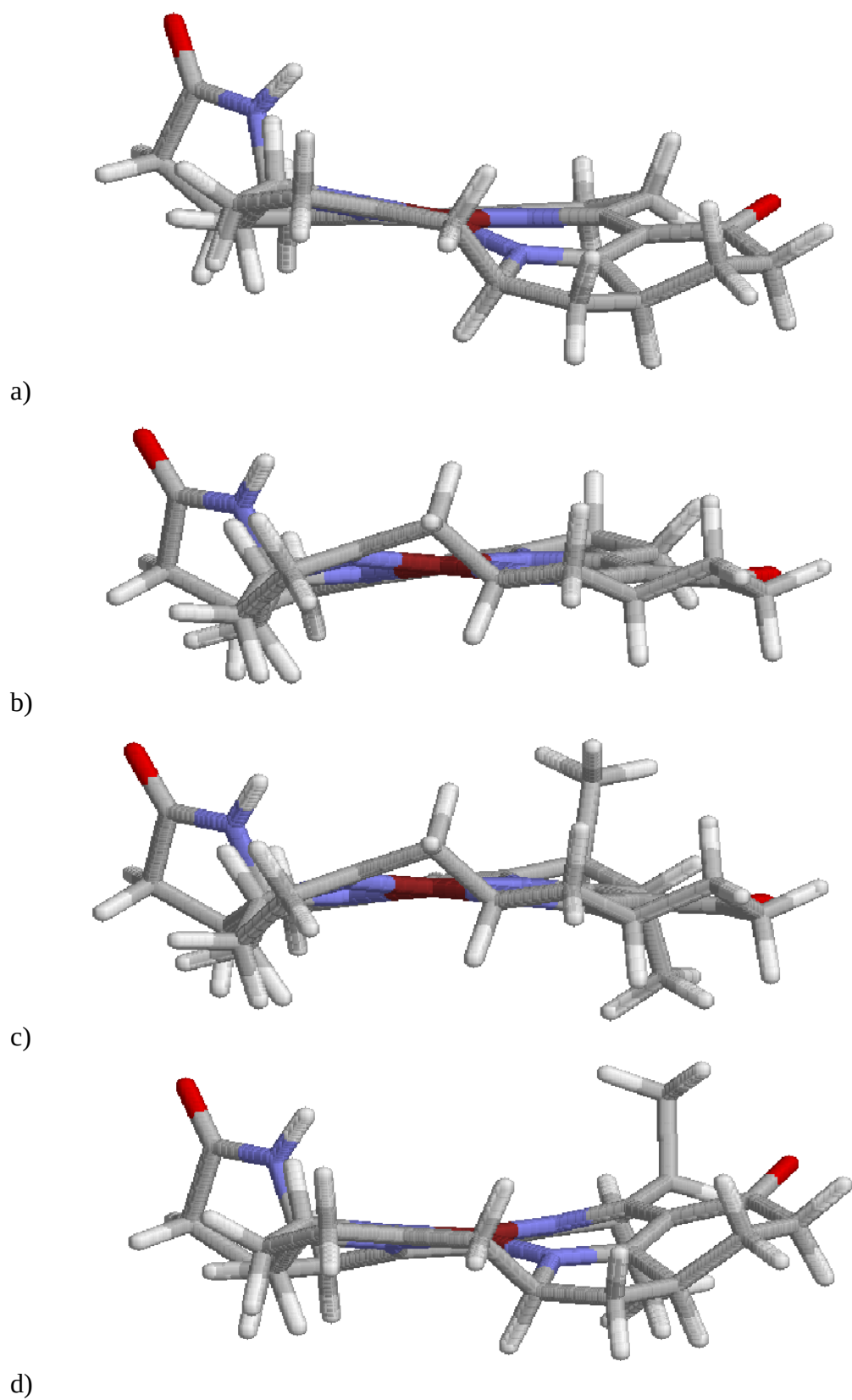
Figure 4. The a) Ibc, b) Chl, and c) Bchl ring systems.

a)

b)

c)
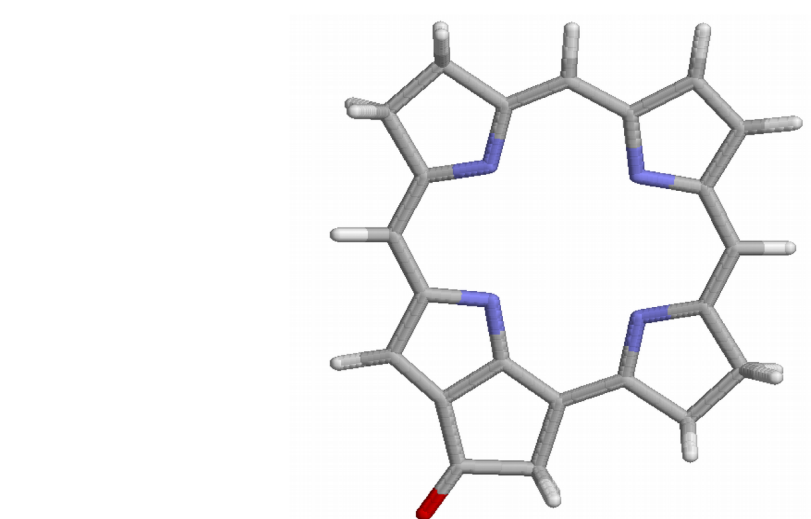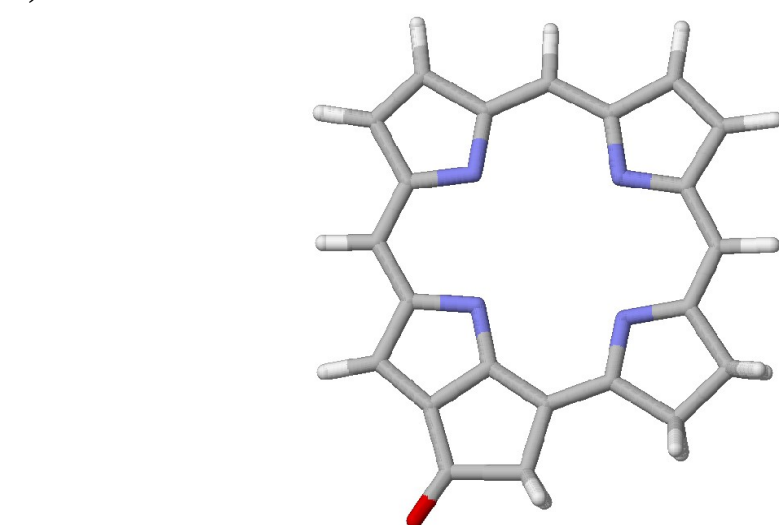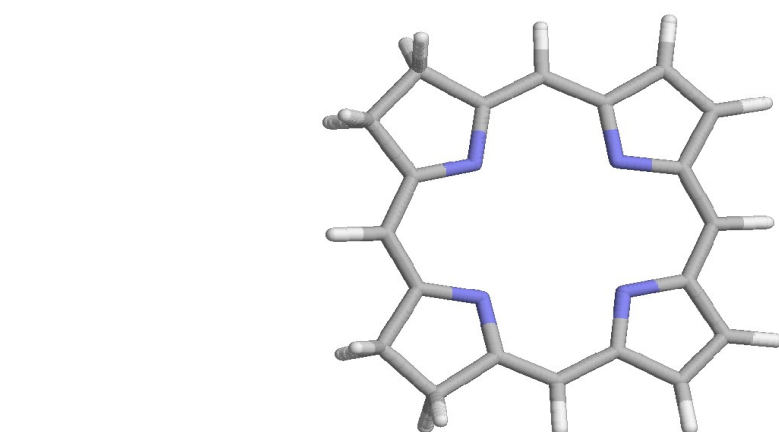
Figure 5. Flexibility in six tetrapyrrole systems, as obtained by relaxed scans of the trans N–N distance.
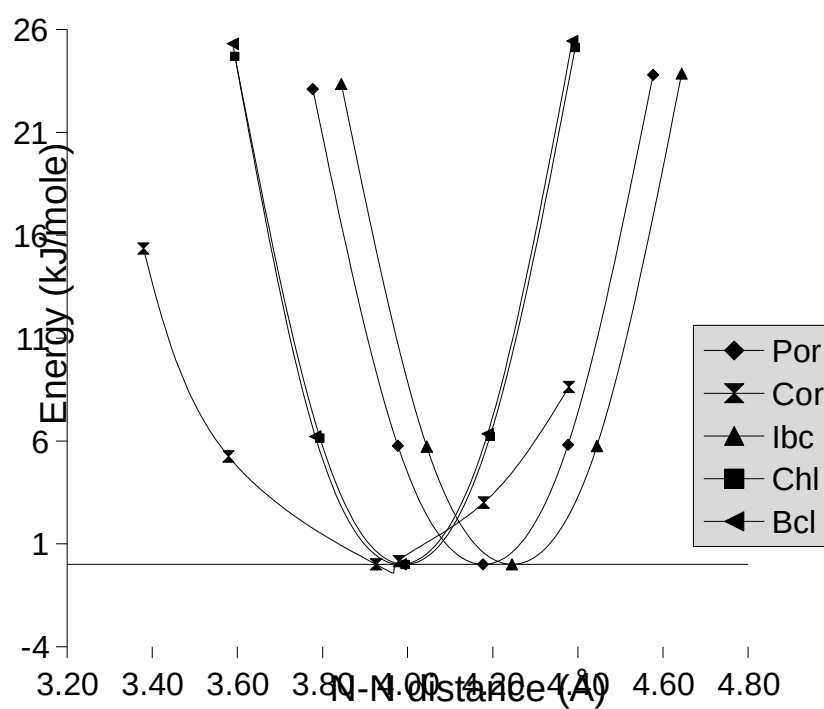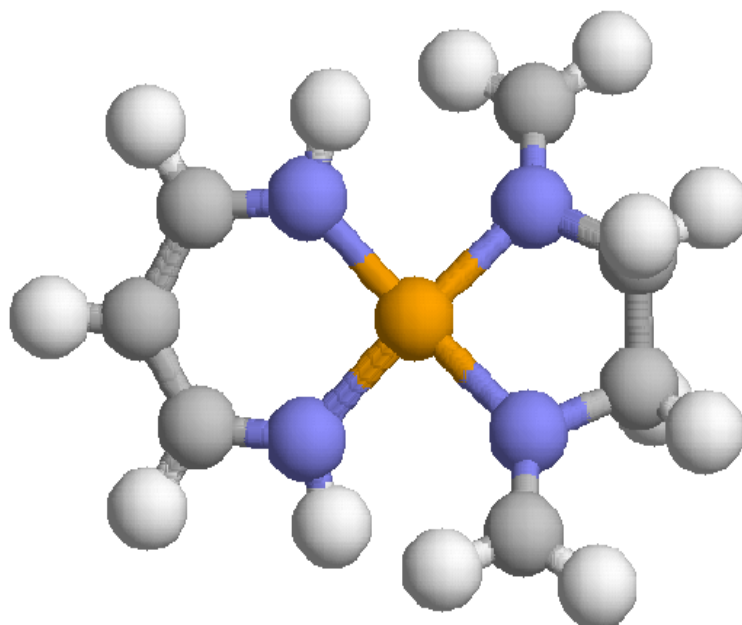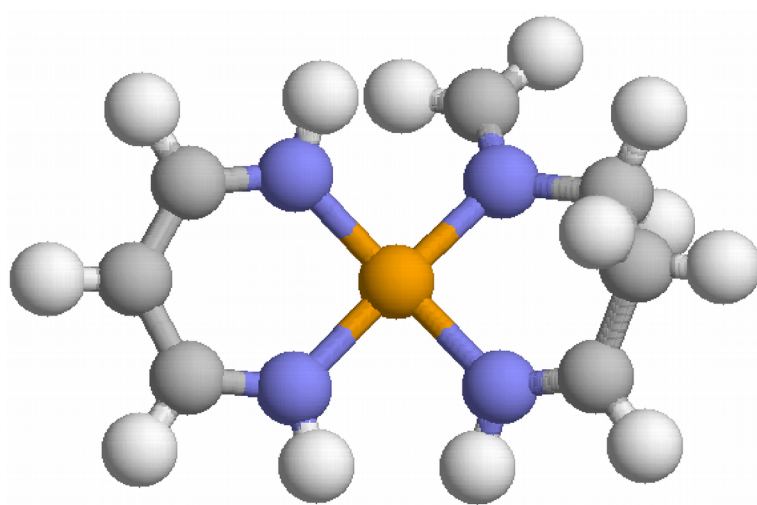

a) Por, Cor, Ibc, Chl, and Bchl
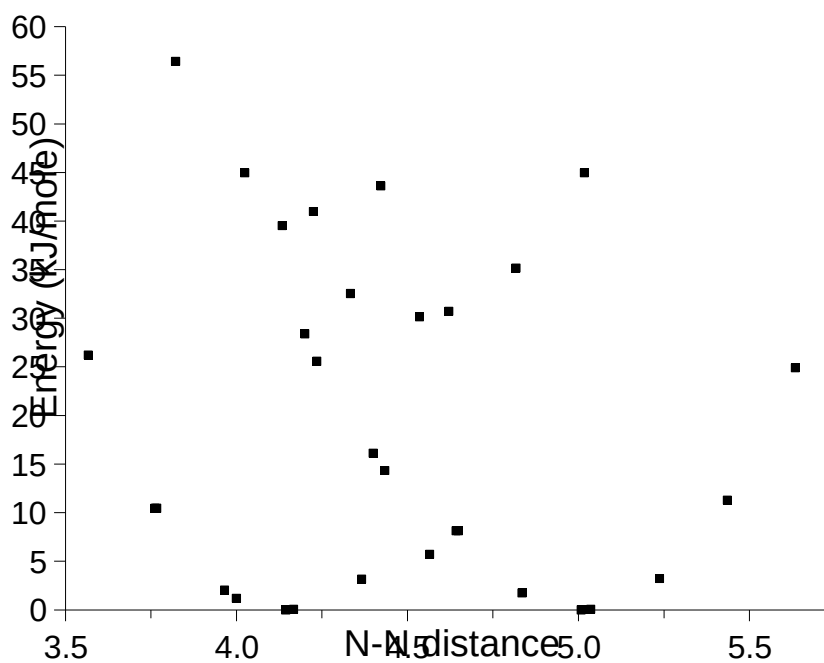
b) Hcor

Figure 6. The $M(NH(CH)_3NH)_2$ and $M(NH(CH)_3NH)(CH_2NH(CH)_2NHCH_2)$ models with removed ring strain.

a) PMod

b) CMod

c) HMod